Climate change increased rainfall associated with tropical cyclones hitting highly vulnerable communities in Madagascar, Mozambique & Malawi

Friederike E. L. Otto[1,*] , Mariam Zachariah[1], Piotr Wolski[2] , Izidine Pinto[2,3], Rondrotiana Barimalala[4] , Bernardino Nhamtumbo[5], Remy Bonnet[6], Robert Vautard[6], Sjoukje Philip[7], Sarah Kew[7], Linh N. Luu[7], Dorothy Heinrich[3], Maja Vahlberg[3], Roop Singh[3], Julie Arrighi[3,8,9], Lisa Thalheimer[10,12], Maarten van Aalst[3,8,11], Sihan Li[12], Jingru Sun[13], Gabriel Vecchi[13,14], Luke J. Harrington[15]

[*]*f.otto@imperial.ac.uk*
[1]*Grantham Institute, Imperial College London, UK.*
[2]*Climate System Analysis Group, University of Cape Town, Cape Town, South Africa.*
[3]*Red Cross Red Crescent Climate Centre, The Hague, The Netherlands.*
[4]*Department of Oceanography University of Cape Town, Cape Town, South Africa.*
[5] *National Institute of Meteorology—INAM, Maputo 256, Mozambique.*
[6] *Institut Pierre-Simon Laplace, CNRS, Sorbonne Université, Paris, France.*
[7]*Royal Netherlands Meteorological Institute (KNMI), De Bilt, The Netherlands.*
[8]*Faculty of Geo-Information Science and Earth Observation (ITC), University of Twente, Enschede, The Netherlands.*
[9]*Global Disaster Preparedness Center, American Red Cross, Washington DC, USA.*
[10]*Princeton School of Public and International Affairs, Princeton University, Princeton, NJ 08540, USA.*
[11]*International Research Institute for Climate and Society, Columbia University, New York, USA.*
[12]*School of Geography and the Environment, University of Oxford, UK.*
[13]*Department of Geosciences, Princeton University, Princeton, NJ 08544, USA.*
[14] *High Meadows Environmental Institute, Princeton University, Princeton, NJ 08540, USA*
[15]*New Zealand Climate Change Research Institute, Victoria University of Wellington, Wellington 6012, New Zealand.*

Madagascar, Mozambique, Malawi and neighbouring countries suffered severe flooding after a series of tropical storms, including three cyclones, hit the region, starting with storms Ana and Batsirai in January and February 2022.

Main findings

- Most impacts were caused by flooding. We therefore assess rainfall associated with tropical storms, measured as the 3-day annual maximum. A measure which is short enough to exclude rainfall from other events that occur close to the event in question but long enough to encompass the full impacts.
- Madagascar, Malawi and Mozambique all had experienced flooding in the weeks preceding Ana, and the communities affected by those floods were left extremely vulnerable to any other hazard, in particular one that compounded the existing flood situations - consecutive tropical storms do not allow people to recover before another one hits. Underlying conditions of conflict (northern Mozambique) and drought (southern Madagascar) likely increased vulnerability. Madagascar is currently grappling with an extreme food insecurity situation, driven by a range of socio-economic conditions and a prolonged drought.
- Both, tropical storm Ana and cyclone Batsirai were well forecasted and tracked notably by Météo Madagascar and the Regional Specialised Meteorological Centre. However, the existence of warnings does not guarantee that these warnings are received and acted upon. In some areas, the damage to communication structures and electrical grids has hampered the reception of the warnings.
- From a meteorological perspective the event (defined in this instance as max. 3-day average rainfall) was only extreme for the first cyclone, Ana, with a return period of approx. 1 in 50 years over Malawi & Mozambique. Batsirai was not a rare event with one of approx. 1 in 2 years over Madagascar.
- Observations of rainfall in the region are sparse and contain many instances of missing data, a quantitative assessment of trends is therefore fraught with uncertainties. Qualitatively, however, in particular taking longer time series into account, an increase in the likelihood and intensity of heavy rainfall as associated with these tropical cyclones can be observed.
- To determine the role of climate change in these observed changes, we combine observations with climate models. We conclude that greenhouse gas and aerosol emissions are in part responsible for the observed increases.
- These findings are consistent with future projections of heavy rainfall associated with tropical cyclones, corroborating the attribution finding that climate change indeed increased the likelihood and intensity of the rainfall associated with Ana and Batsirai.

1 Introduction

The Southwest Indian Ocean, including the Mozambique Channel is a recognized hotspot of tropical storms and cyclones, and associated with significant loss and damage in the areas hit. In late January, Tropical Storm Ana brought winds, heavy rains, damage and destruction to parts of Madagascar, Mozambique, Malawi and Zimbabwe. Ana was followed by Tropical Cyclone Batsirai hitting the South coast of Madagascar on February the 5th 2022. Ana and Batsirai were the first storms of the 2021-22 Southwest Indian Ocean cyclone season (November-April) and affected several hundred thousand people across the affected countries. Following those two storms three weaker storms, Dumako, Emnati, and Gombe also made landfall that led to further flooding and casualties.

The circulation system of Ana was a tropical depression when it passed through east of Madagascar on 22 January 2022. However, the region was already reeling under floods and casualties from heavy rainfall spells in the preceding week, associated with the annual southward migration of the Inter-Tropical Convergence Zone (ITCZ) , thereby compounding the impacts. Although the system had weakened into a tropical disturbance when exiting the island on 23 January 2022, it started strengthening again while moving across the Mozambique Channel, finally making landfall in Mozambique on 24 January 2022 as a moderate tropical storm.
Batsirai's effects were primarily over Madagascar, where the cyclone made landfall as a Category 3 storm on 5 Feb 2022 on the east coast. Heavy rainfall and strong gusts continued till 7 Feb 2022 as it moved southwest across the island and weakened into a remnant low.

Both Ana and Batsirai caused severe humanitarian impacts in Madagascar, Mozambique, and Malawi including deaths and injuries, infrastructure damage, and a range of long-lasting socio-economic impacts which may become even more apparent as the recovery process begins. The impacts were further compounded by preceding flood events and in Southern Madagascar a severe drought.

Malawi and Mozambique strongly felt the impacts of Ana as it made landfall on the Mozambique coastline and moved inland. In Mozambique, over 141,483 people are estimated to have been directly affected, including at least 25 deaths (OCHA, 2022a). In Malawi, over 945,728 people are estimated to have been impacted by Ana including nearly 40,000 children under-five, more than 10,000 people living with disabilities and roughly 21,000 pregnant and lactating women (IFRC, 2022a), as well as over 190,429 displaced by the storm (IFRC, 2022b) and 46 accounted dead (OCHA, 2022b).

Storm Ana had significant impacts on infrastructure and land. In Mozambique, more than 7,700 homes and 2,457 classrooms were reportedly destroyed, 70,982 hectares of land flooded, 23 water supply systems, 144 power poles and 2.275 km of roads damaged (OCHA, 2022a). In Malawi, reported impacts include over 476 schools damaged, roads damaged, bridges washed away and churches damaged (Ibid.), heavily reduced power generation capacity, failure to operate water treatment and distribution systems including over 1,000 boreholes damaged,

contaminated or filled, impacting the access to potable water for over 300,000 people (OCHA, 2022b). In addition, the aftermath of Storm Ana is already showing important socio-economic impacts notably on agricultural communities with many crops lost to the floods and winds. Notably, over 37,000 hectares of crops were flooded in Mozambique (OCHA, 2022a) and 115,388 hectares in Malawi (IFRC, 2022b). Health impacts were also a concern in both Mozambique and Malawi notably due to the damage of 30 healthcare facilities in Mozambique (OCHA, 2022a) and 47 in Malawi (OCHA, 2022b). Additional reports of negative impacts on nutrition and generalised food insecurity, particularly for already vulnerable groups such as children and the elderly as well as increased exposure to protection risks for women and girls (IFRC, 2022b; UNICEF, 2022). All this also happened in the context of the Covid-19 pandemic, with additional risks of cholera and polio outbreaks, measles, and malaria being of particular concern (OCHA, 2022b; WHO, 2022). In addition, Madagascar is already grappling with severe food insecurity (see Harrington et al., 2021).

In Madagascar, storm Ana is estimated to have affected over 500,000 people (OCHA, 2022c) including 72,000 people displaced (Windsor, 2022) and tens of thousands left without electricity (France 24, 2022). The official death toll sits around 58 (OCHA, 2022d). Only a week later, Cyclone Batsirai came as a rapid compound event in a country already coping with the recovery from storm Ana. In Madagascar, the death toll from Batsirai was much higher than for storm Ana, with official numbers around 120 (OCHA, 2022e) including 87 people from the Ikongo district, in the south-west of the country, alone (Rabary, 2022).

After Batsirai, over 20 roads and 17 bridges were recorded as destroyed, which left the worst-affected areas inaccessible by road (Al Jazeera, 2022). At least 10,900 homes were damaged or completely destroyed (ECHO, 2022) and 69 health care centres were damaged (CARE, 2022). The city of Manajary was particularly devastated. In addition, increased food prices (notably for rice) were also reported in Mozambique in the aftermath of Batsirai and Ana (MSF, 2022). Given the highly stressed situation in the region in the past seasons and years, there is elevated concern about heightened food insecurity (FEWSNet, 2022). Finally, many health impacts are being felt as Madagascar recovers from both storms, including an increased number of cases of diarrhoea and respiratory infections reported by Médecins Sans Frontières (MSF, 2022).

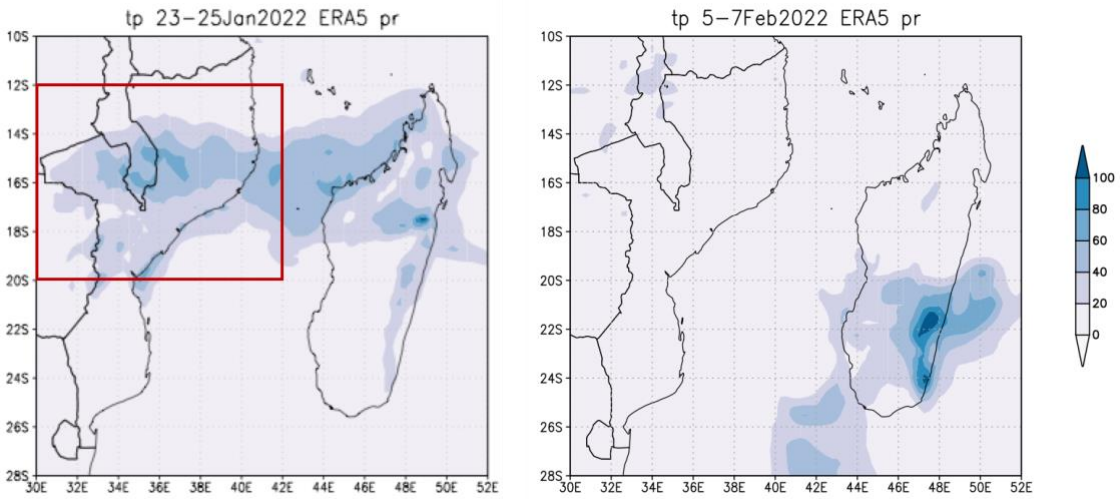

Fig1. 3-day average precipitation [mm/day] from tropical storm Ana (left) and tropical cyclone Batsirai (right) in ERA5 reanalysis data. The red box indicates the region used for the assessment in Mozambique and Malawi.

The impacts from both these storms in the affected regions were primarily driven by the heavy precipitation the storms brought, causing widespread flooding that led to subsequent infrastructure damage and loss of lives. Therefore, accumulated or averaged precipitation for typical durations of tropical storms (or cyclones) in the region in question is the variable most closely connected to the impacts and is used for discerning the role of climate change in this attribution study. To determine the temporal scale of the event, we need to ensure that the period is sufficiently long to capture the rainfall associated with the storm over a particular location while short enough to not include rainfall due to other phenomena. Therefore, this period is fixed at 3 days for this study, a justified choice given that this is the average duration over which these events persisted over the affected areas.

Fig. 1 shows the 3-day average rainfall over the Madagascar and Mozambique Channel from Ana and Batsirai. Based on the respective areas over which the impacts from these storms were greatest, two spatial domains are identified for this study, as follows:

1. A box (see Fig. 1(*left)*) over Mozambique and Malawi [20S-12S; 30E-42E]- the MM-box, for Tropical Storm Ana, and
2. Madagascar as a whole, for Cyclone Batsirai.

Fig. 2 shows the area-averaged annual precipitation cycles for Madagascar (Fig. 2(a-c)) and the MM-box (Fig. 2(b-d)), for three available gridded observational datasets. The cycles for both the regions follow unimodal distributions with most of the precipitation occurring during the cyclone season of November-April, and peaking in January. We therefore choose to look for annual extreme events, defining the year as July-June.

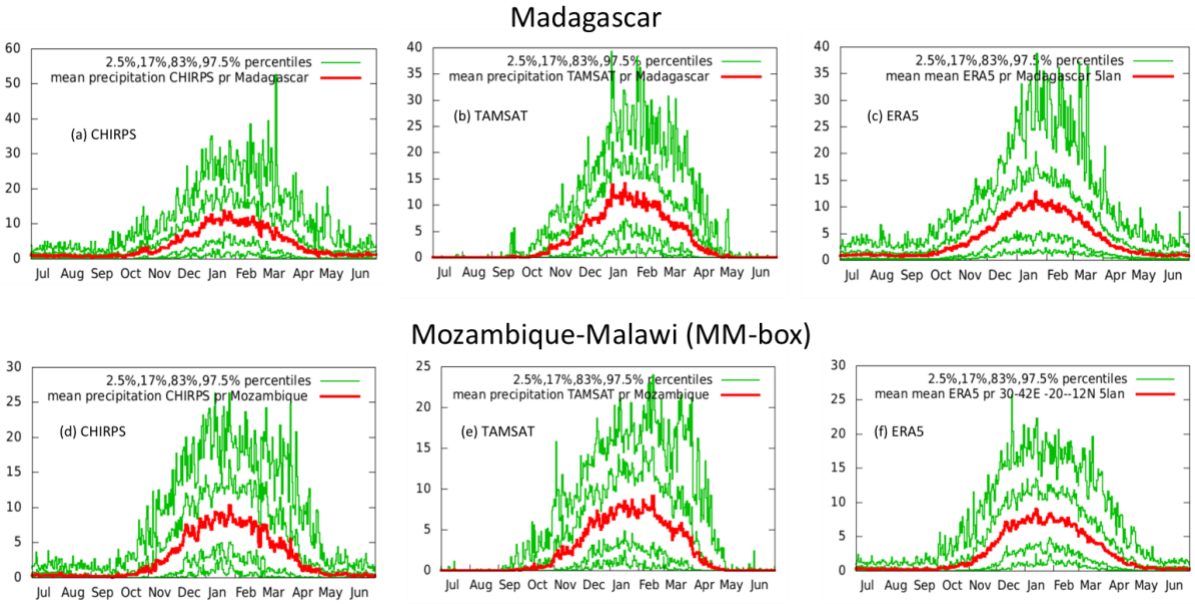

Fig2. Area-averaged annual precipitation cycles (mm/day) based on CHIRPS, TAMSAT and ERA5 datasets for Madagascar (top) and the MM-box (bottom).

Further, we examine the sensitivity of the choice of 3-day precipitation averaging period in reflecting the impacts of storms in the selected domains. Fig. 3 shows the 3-day accumulated precipitation series over Madagascar and the MM-box, also highlighting the precipitation associated with cyclone events (black dots, from IBTrACS[1]) in the respective regions. A substantial proportion - about 65% - of the annual 3-day precipitation maxima over Madagascar are found to be frequently associated with cyclones. This fraction is somewhat less (22%) for the MM-box.

This implies that in this study we take into account trends in heavy precipitation more generally, not limited to trends in precipitation associated with tropical cyclones only. However, tropical depressions, a major cause of heavy rainfall events in the area, have very similar synoptic features to cyclones, but are not captured by cyclone tracking datasets. If these were included the proportion of tropical storm-related heavy rainfall events were even higher. We thus consider the 3-day annual max rainfall as an impact-relevant indicator for flood-damage during the tropical cyclone season.

[1] https://climatedataguide.ucar.edu/climate-data/ibtracs-tropical-cyclone-best-track-data

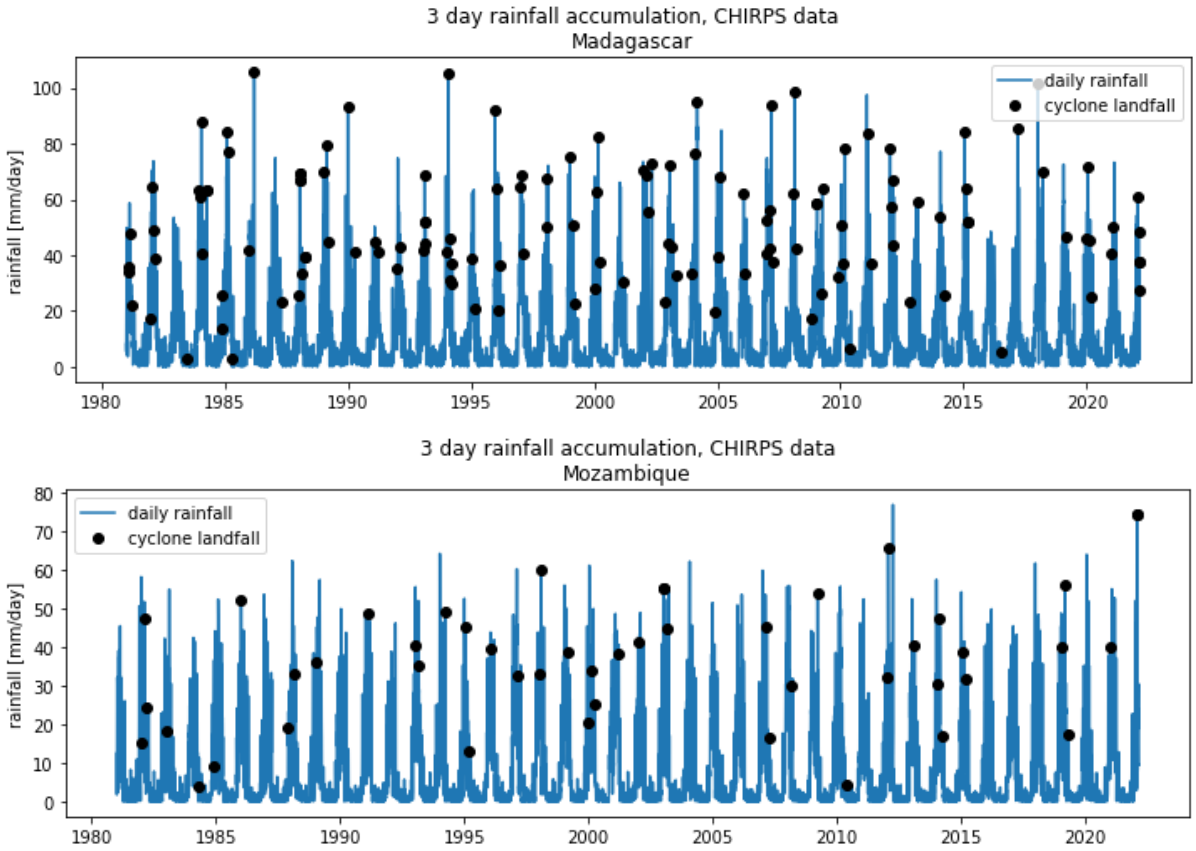

Fig3. Area-averaged 3-day running accumulated precipitation series for Madagascar (top) and the MM-box (bottom). The black dots highlight the instances where the precipitation is associated with a cyclone event (from the IBTrACS dataset). Data: CHIRPS

Tropical storms and cyclones are an annual occurrence in Madagascar, Mozambique, and Malawi in this season. Between 1986 and 2021, the EM-DAT[2] database reported that a cumulative 96 tropical storms have hit the three countries. Based on gridded observational data assessment (see section 3.2) the precipitation associated with storm Ana had a return period of 1 in 50 years, so clearly and extreme event, while Batsirai was a 1 in 2 year event (ie. with a 50% chance of occurring every year), not very extreme for Madagascar. Looking at station data alone (see section 3.1) also the rainfall in Mozambique was on the order of a 1 in 2-6 year event. In terms of impacts, which were driven mostly by flooding, both storms were not that unusual. For example, according to EM-DAT, 40% of storms to have hit either of the three countries since 1968 have had death tolls over 25, and 30% over 50. Although the impacts of tropical storms in the region are not particularly unusual, this level of impact *is* considered extreme at a global scale, at a level which triggered the WWA protocol (>100 deaths and >1,000,000 people affected, reaching 2/3 of the threshold). The vulnerability and exposure contexts of the region (see section 7) partially explains this pattern.

There is relatively little literature on the influence of anthropogenic climate change on tropical cyclones and storms over basins other than the North Atlantic. The IPCC AR6 report

[2] https://www.emdat.be/database

(Seneviratne et al., 2021) states low confidence in most reported long-term (multidecadal to centennial) trends in tropical cyclone frequency- or intensity globally when all types of tropical cyclones are considered. This lack of evidence should not be interpreted as implying that no trends exist, but rather as indicating that either the quality or the temporal length of the data is not adequate to provide robust assessments. The AR6 further states that it is however likely that the proportion of major tropical cyclone intensities and the frequency of rapid intensification events have both increased globally over the last 40 years. An increase in the occurrence of the most intense tropical cyclones has also been observed over the South Indian Ocean (SIO; Kossin et al., 2020).

To our knowledge there are no attribution studies, linking these observed trends to anthropogenic climate change. There is further limited evidence from individual event attribution studies on the intensification of tropical cyclones (Patricola & Wehner, 2018). There is much more robust evidence that anthropogenic climate change contributed to extreme rainfall amounts during several intense tropical cyclones and storms in the North Atlantic (e.g Emanuel, 2017; van Oldenborgh et al., 2017 and Risser and Wehner, 2017) and outside, leading the AR6 to conclude with high confidence that precipitation intensities associated with tropical storms have increased. This statement is however a global average, and as with other types of extreme events, including heat waves, local changes can be different. Luu et al. (2021) found a limited role for global warming in the heavy rainfall associated with recent typhoons in Vietnam. Given the lack of any attribution studies on any aspects of tropical cyclones hitting the African continent, despite repeated devastating landfalls in recent years, a dedicated attribution study is needed to identify whether and to what extent tropical cyclones in the Mozambique channel differ from the globally expected picture.

Rainfall associated with tropical cyclones is projected to increase further with warming following the Clausius-Clapeyron relationship on average, but with several regions expected to see higher rain rates, especially on daily and shorter timescales (Seneviratne et al., 2021). Tropical cyclone tracks and the location of topography relative to the cyclones significantly affect precipitation, thus in general, areas on the eastern and southern faces of mountains have higher precipitation changes.

2 Data and methods

2.1 Observational data

Daily rainfall observations for 24 stations (Fig. 4) in the study domain were made available by the Mozambique National Institute of Meteorology. However, only 4 stations have the quality (low proportion of gaps) and length (1981-2022) required for assessing trends (as shown in appendix Fig. A1). Even these observations are too short to draw defensible attribution conclusions or evaluate the quality of the gridded data products over the relatively large study domain. Therefore, we use the data only in a limited manner - as an independent

line of evidence and a source of cross-validation for the generalised extreme value (GEV) distribution parameters used in analyses of gridded data (see section 3.1).

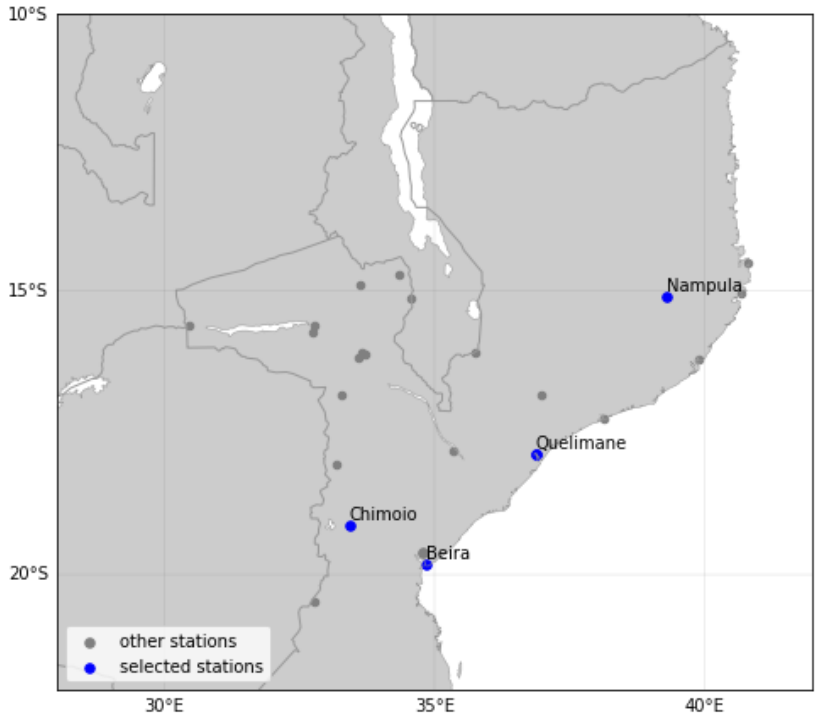

Fig4. Weather stations within the region of the MM-box. The four stations with relatively few days of missing data since 1981 are marked in blue.

We use three gridded datasets for fitting probability distributions to rainfall in the study region(s) and thereafter analysing the heavy rainfall event due to Ana and Batsirai in the context of climate change. The first dataset is the rainfall product developed by the Tropical Applications of Meteorology using Satellite data and ground-based observations (TAMSAT) group at the University of Reading, UK, based on high-resolution Meteosat thermal infrared (TIR) imagery that are calibrated using rain gauge observations (Maidment et al., 2014, 2017; Tarnavsky, 2014). The rainfall product developed by the UC Santa Barbara Climate Hazards Group called "Climate Hazards Group InfraRed Precipitation with Station data" (CHIRPS; Funk et al. 2015) is the second dataset considered in this study. Both products have wide applications in weather monitoring and forecasting and crises management in Africa by engaging with the various government agencies (see http://www.tamsat.org.uk/impact; https://www.chc.ucsb.edu/monitoring). However, both these products have relatively shorter lengths, starting at 1983 and 1981, respectively, which leads to very high uncertainties in the estimated precipitation trends. Therefore, we also include data from the European Centre for Medium-Range Weather Forecasts- the ERA5 reanalysis product , which is longer in length (starting at 1950). We note that precipitation from ERA5 is not directly assimilated, but it is a diagnostic variable generated by atmospheric components of the IFS modelling system. For the period prior to 1979, the information on tropical cyclones best track minimum mean sea level pressure is assimilated to have a better representation of the extremes (Hersbach et al. 2020).

For obtaining rainfall distributions with respect to a hypothetical climate devoid of anthropogenic influence, we assume that the distribution parameters scale with the Global Mean Surface Temperature (GMST), an accepted measure of anthropogenic climate change (e.g., Luu et al., 2021; van Oldenborgh et al., 2017). We use low-pass filtered estimates of annual global mean surface temperature (GMST) from the National Aeronautics and Space Administration (NASA) Goddard Institute for Space Science (GISS) surface temperature analysis (GISTEMP, Hansen et al., 2010 and Lenssen et al. 2019).

2.2 Model and experiment descriptions

In addition to the observed datasets, we use three different ensembles from climate modelling experiments using very different framings (Philip e al., 2020): SST driven global circulation models, coupled global circulation models and regional climate models..

The first ensemble is the HighResMIP SST-forced model ensemble (Haarsma et al. 2016), the simulations for which span from 1950 to 2050. The SST and sea ice forcings for the period 1950-2014 are obtained from the 0.25° x 0.25° Hadley Centre Global Sea Ice and Sea Surface Temperature dataset that are area-weighted regridded to match the climate model resolution (see Table 1). For the 'future' time period (2015-2050), SST/sea-ice data are derived from RCP8.5 (CMIP5) data, and combined with greenhouse gas forcings from SSP5-8.5 (CMIP6) simulations (see Section 3.3 of Haarsma et al. 2016 for further details).

The second ensemble considered in this study is GFDL-CM2.5/FLOR. This is a fully coupled climate model developed at the Geophysical Fluid Dynamics Laboratory (GFDL; Vecchi et al., 2014) with horizontal resolution of 50 km for land and atmosphere and 1 degree for ocean and ice. The five ensemble simulations cover the period from 1860 to 2100, and include both the historical and RCP4.5 experiments driven by transient radiative forcing from CMIP5 (Taylor et al., 2012).

The third ensemble is the CORDEX-Africa (0.44° resolution, AFR-44) multi-model ensemble (Nikulin et al., 2012), comprising of 23 simulations resulting from pairings of Global Climate Models (GCMs) and Regional Climate Models (RCMs). These simulations are composed of historical simulations up to 2005, and extended to the year 2100 using the RCP8.5 scenario.

The 1950-2022 period for which the observed data is available is chosen for model evaluation, while the entire length of simulations up to the year 2022 is considered for the attribution analysis.

Model	Resolution	Institute
CMCC-CM2-VHR4	~25 km	Fondazione Centro Euro-Mediterraneo sui Cambiamenti Climatici
CMCC-CM2-HR4	~100 km	Fondazione Centro Euro-Mediterraneo sui Cambiamenti Climatici
CNRM-CM6-1-HR	~50 km	Centre National de Recherches Meteorologiques
CNRM-CM6-1	~100 km	CNRM-CERFACS
EC-Earth3P-HR	~40 km	EC-Earth-Consortium
EC-Earth3P	~80 km	EC-Earth-Consortium
HadGEM3-GC31-HM	~25 km	UK Met Office, Hadley Centre
HadGEM3-GC31-MM	~60 km	UK Met Office, Hadley Centre
MPI-ESM1-2-XR	~60 km	Max Planck Institute for Meteorology
MPI-ESM1-2-HR	~100 km	Max Planck Institute for Meteorology

Table 1. List of HighResMIP models used in the study.

2.3 Statistical methods

In this study we analyse area averaged precipitation time series for Madagascar and the MM-box (see Fig. 1). Methods for observational and model analysis and for model evaluation and synthesis are based on the World Weather Attribution Protocol, described in Philip et al. (2020), with supporting details found in van Oldenborgh et al. (2021), Ciavarella et al. (2021) and here.

The analysis steps include: (i) trend calculation from observations; (ii) model evaluation; (iii) multi-method multi-model attribution and (iv) synthesis of the attribution statement.

We calculate the return periods, Probability Ratio (PR) and change in intensity of the event under study for the comparison between observed GMST values of 2022 and past GMST values (1850-1900, based on the Global Warming Index https://www.globalwarmingindex.org), which is a difference of 1.2 °C.

3 Observational analysis: return time and trend

Several options exist when evaluating a recent extreme weather event in the context of historical climate observations. While analysing historical data from local weather stations is the first preference for any study, there are only very few stations of sufficient quality within the regions of interest. In Madagascar and Malawi there are no suitable stations, but, as described above, there are some in Mozambique. The main analyses are based on the gridded data sets as described above, but we use the four usable stations in Mozambique as an additional line of evidence for the MM-box region assessment.

3.1 Analysis of point station data

Fig. 5 shows the trend fitting methods described in Philip et al. (2020) applied to the transient series of annual maximum 3-day average rainfall, for the four stations identified above (sec. 2.1). The behaviour of the location parameter with respect to the GMST (Fig.5 (*left*)) suggests an increase in average rainfall due to warming, for all stations except Quelimane. Further, the return period of 2022 rainfall in the current climate is found to range from 1 to 18 years for these stations (Fig. 5 (right)), which is much lower than the estimate of 50 years adopted for Mozambique, based on gridded data analysis, as explained in the next section. Although we cannot compare an area average directly with station data, these results corroborate the finding that the event is not very extreme from a meteorological point of view.

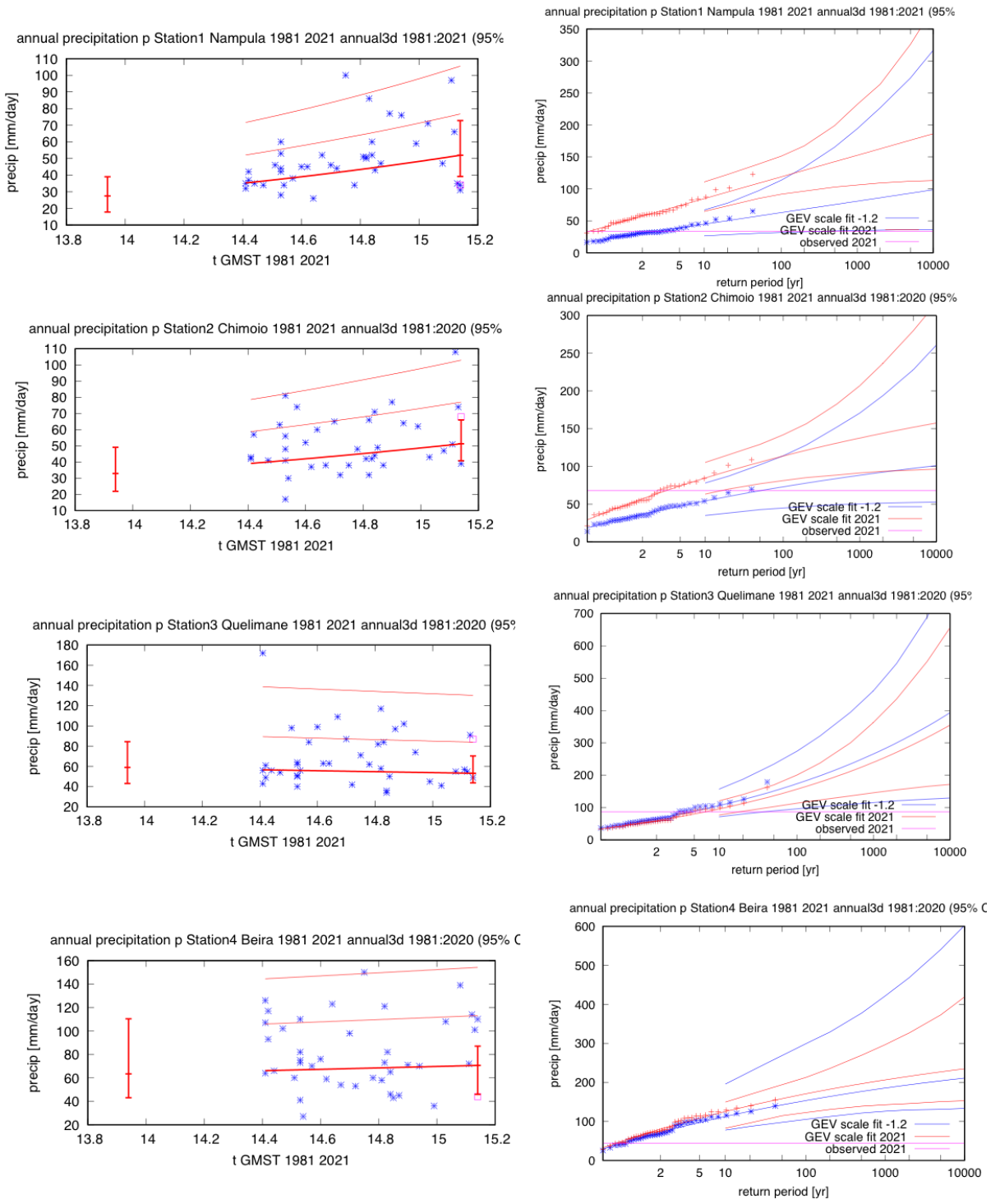

Fig5. *GEV fit with constant dispersion parameters, and location parameter scaling proportional to GMST of the index series, for the four weather stations in Mozambique. No information from 2022 is included in the fit.* ***Left****: Observed max. annual 3-day average rainfall as a function of the smoothed GMST. The thick red line denotes the time-varying location parameter. The vertical red lines show the 95% confidence interval for the location parameter, for the current, 2022 climate and the fictional, 1.2ºC cooler climate. The 2022 observation is highlighted with the magenta box.* ***Right****: Return time plots for the climate of 2021/22 (red) and a climate with GMST 1.2 ºC cooler (blue). The past observations are*

shown twice: once shifted up to the current climate and once shifted down to the climate of the late nineteenth century. The markers show the data and the lines show the fits and uncertainty from the bootstrap. The magenta line shows the magnitude of the 2022 event analysed here.

3.2 Analysis of gridded data

Fig. 6 shows the precipitation time-series for CHIRPS (1981-present), TAMSAT (1983-present)and ERA-5 (1950-present) for Madagascar (Fig. 6 (top)) and the MM-box (Fig. 6 (bottom)). Overall, these records are in agreement, showing increasing trends in annual maximum rainfall, for both regions. We acknowledge that ERA5 is found to be biased slightly wet for some parts of Africa (Gleixner et al., 2020; Terblanche et al., 2021) and the other data sets are developed for the region. However, the length of the other two data sets are too short to identify significant trends in a noisy measure. We thus use all three datasets (Fig. 6), seasonal cycles (Fig. 2) and spatial patterns (Fig. 10) as interchanegable sources for computing return periods of the storm events, as follows.

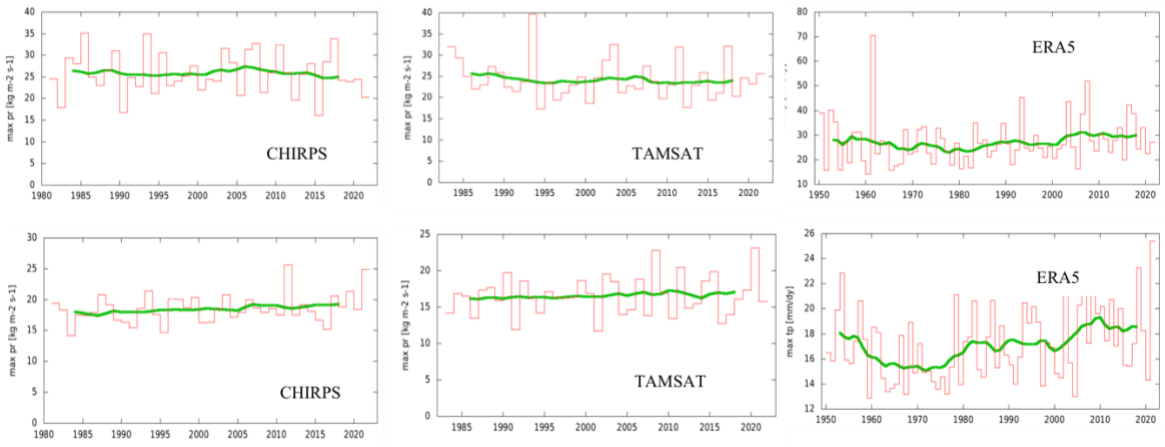

Fig6. *Time series of annual (July-June) maxima of 3-day average rainfall along with the ten-year running mean (shown by green line) for Madagascar (top) and Mozambique (bottom), based on CHIRPS, TAMSAT and ERA5 rainfall datasets.*

As with station-based observations, the left panels in Fig. 7 show the response of annual maximum 3-day average precipitation to the global mean temperature, for Madagascar, based on the gridded datasets from CHIRPS, TAMSAT and ERA5 (similar plots for the MM-box in Fig. 8). The right panels in Figs. 7 & 8 show the return period curves in the present, 2022 climate and the past climate when the global mean temperature was 1.2 °C cooler. Because the TAMSAT and CHIRPS time series are too short to obtain the return period with enough confidence, we use the return periods from ERA5 for the model analysis. These are, for the current climate, rounded to 2 years for Madagascar and 50 years for the MM-box.

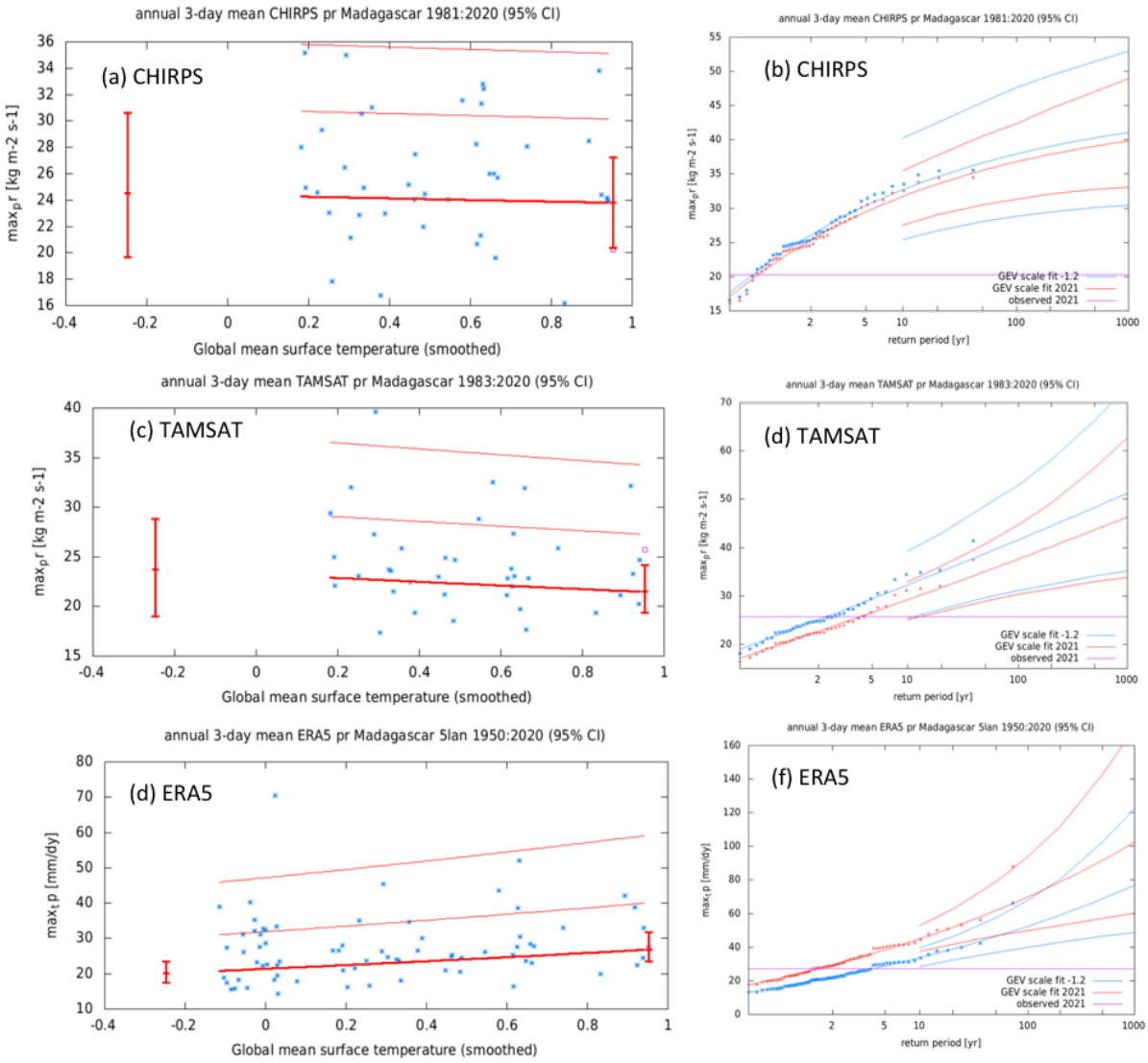

Fig7. *same as Fig. 5, but for Madagascar, based on observed data from CHIRPS (**top**), TAMSAT (**middle**) and ERA5 (**bottom**).*

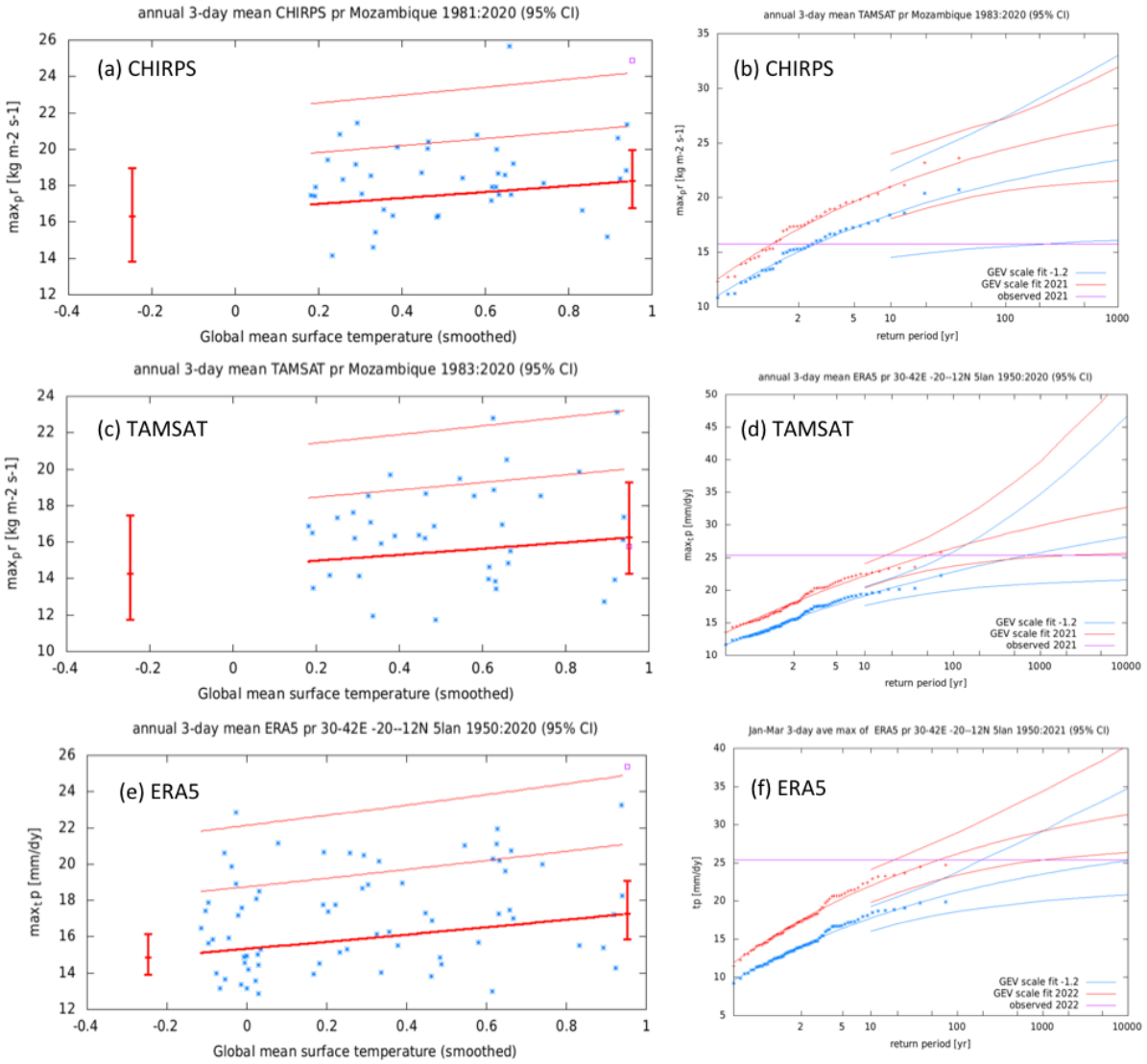

Fig8. *same as Fig. 5, but for the MM-box, based on observed data from CHIRPS (**top**), TAMSAT (**middle**) and ERA5 (**bottom**).*

3.3 Influence of modes of natural variability

Tropical and subtropical teleconnections, particularly the El-Niño Southern Oscillation (ENSO) is a principal driver of rainfall variability in sub-Saharan Africa (Camberlin et al., 2001) and cyclonic activity in the adjoining seas (Burns et al., 2016). Fig. 9 shows the timing of wet and dry seasons associated with the negative phase of ENSO or *La-Niña*, for the various global regions. During austral summer (November-April), this phase fosters positive rainfall anomalies in the southern part of Africa including the study domain, by influencing the locations of major circulations responsible for synoptic rainfall-mechanisms in these regions, primarily, the South Indian Convergence Zone (SICZ; Hoell et al., 2015; Hart et al., 2018) and the Intertropical Convergence Zone (ITCZ; Schneider et al., 2014).

On the other hand, the association between ENSO and cyclonic activity in the Southwest Indian Ocean is not as straightforward, and therefore not conclusive. Some features of positive ENSO phase or *El-Niño*, primarily high SSTs and humidity that are conducive for cyclogenesis are countered by other *El-Niño* features such as strong vertical westerly shear and weak upper layer, anti-cyclonic vorticity (Burns et al., 2016; Mavume et al., 2009). Consequently, cyclonic activity is slightly higher in the *La-Niña* years.

The 2022 cyclone season was accompanied by La Niña conditions persisting into the second consecutive year, which has been shown to have influenced above-average rainfall seasons over southern Africa[3]. However, the extent to which these modes of variability represent a causal driver of specific rainfall events, in particular also over Madagascar which is outside the region typically influenced, remains less clear. Further, there is evidence of climate change intensifying precipitation rates during tropical cyclones in these regions (Knutson et al., 2015), alongside decreases in cyclone activity (Muthige et al., 2018; Cattiaux et al., 2018). Therefore, attribution studies focusing on precipitation associated with storms and thus including both effects are useful to understand the overarching role of climate change in one of the most damaging aspects of tropical cyclones.

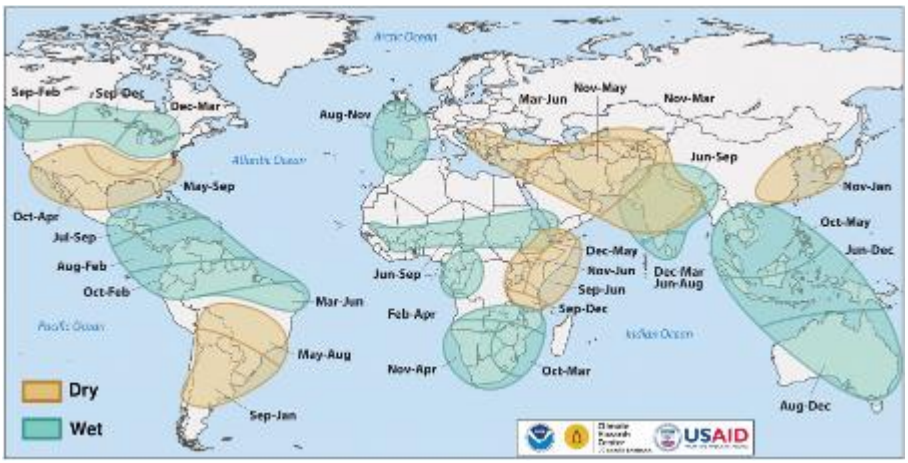

Fig9. *Schematic illustrating the timing of wet and dry conditions related to La Niña (source https://fews.net/la-niña-and-precipitation)*

[3] https://docs.wfp.org/api/documents/WFP-0000133106/download/

4 Model evaluation

We use three criteria to assess the models' fitness for purpose. Firstly, we qualitatively compare the seasonal cycles in models and observations; secondly, we compare the spatial pattern of annual rainfall and thirdly, we compare the parameters of the fitted GEV in observations and models. The assessment of whether the seasonal cycles in the models follow the observed cycles (see Fig. 2) is done by visually inspecting the mono-modal distributions. For the spatial patterns we compare, again visually, the annual mean rainfall in the observations (Fig. 10) with those in the models. Many models show very high levels of rainfall over the Mozambique channel and are excluded from the analysis.

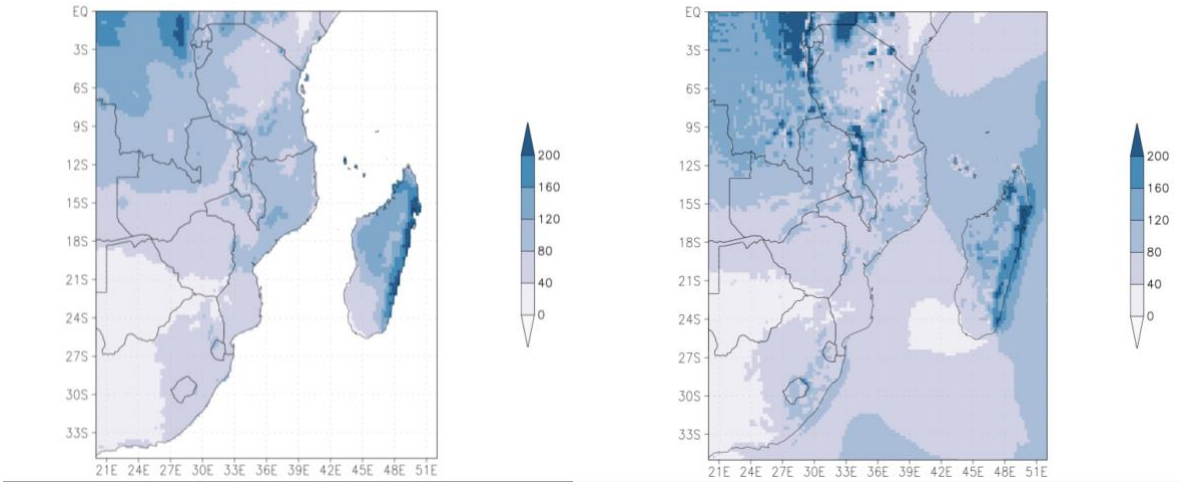

***Fig10**. Annual average daily mean precipitation pattern (mm/day) for CHIRPS (left) and ERA-5 (right) averaged over the length of the respective time series.*

The figures for patterns and seasonal cycles in the models can be found in the appendix. Fig. A2 shows the annual precipitation cycles based on CORDEX models for Madagascar (Fig. A3 shows similar plots for the MM-box). The average precipitation patterns over the larger domain including both Madagascar andt the MM-box, based on these models are shown in Fig. A4. Figs A5-A6 show the seasonal cycles and spatial pattern of precipitation from the coupled FLOR model.

Fig. A4 shows that many models have a large bias over the Mozambique Channel. Because of the large discrepancies in the observed rainfall distributions in the different observational data products, the spatial pattern assessment in particular provides a harder test for the models.We note however, that because of the difficulty in assessing reliable observations, models labelled "good" would more realistically be labelled "not terrible" as all criteria are comparably weak.

Tables 2 &3 show the model evaluation results, including both the models that passed the evaluation tests (labelled as "good", green) and models which did not (labelled as "reasonable" (yellow) "bad", red). Of those models considered, all that were labelled as "bad"

or “reasonable” were discarded from the subsequent attribution analysis, for either of three reasons, the spatial patterns of the rainfall did not resemble those of the observations, the seasonal cycle is wrong, or the 95% confidence intervals of the GEV parameters did not overlap with the corresponding confidence intervals in the observational data sets. We also note that values for CHIRPS and TAMSAT in Table 1 are very different to those of ERA5. The statistical test thus only offers limited insight into the fitness for purpose of the models.

Observations	**Seasonal cycle**	**Spatial pattern**	**Dispersion**	**Shape parameter**	**Event magnitude**
CHIRPS			0.107 (0.0730 ... 0.125)	-0.10 (-0.43 ... 0.099)	24.9
TAMSAT			0.157 (0.117 ... 0.184)	-0.17 (-0.45 ... 0.036)	15.8
ERA5			0.141 (0.114 ... 0.160)	-0.086 (-0.31 ... 0.14)	25.4
Model					**Threshold for 50-yr return period**
CMCC-CM2-VHR4 HighResMIP (1)	good	bad	0.170 (0.137 ... 0.198)	0.15 (0.0050 ... 0.29)	36.3
CNRM-CM6-1-HR HighResMIP (1)	good	reasonable	0.215 (0.174 ... 0.248)	-0.011 (-0.15 ... 0.11)	27.8
EC-Earth3P-HR HighResMIP (1)	good	good	0.131 (0.110 ... 0.146)	-0.020 (-0.27 ... 0.11)	25.4
HadGEM3-GC31-HM HighResMIP (1)	good	good	0.151 (0.124 ... 0.172)	-0.053 (-0.23 ... 0.092)	31.7
MPI-ESM1-2-XR HighResMIP (1)	good	good	0.101 (0.0830 ... 0.115)	-0.096 (-0.27 ... 0.046)	18.3
HadGEM3-GC31-MM HighResMIP (1)	good	bad	0.167 (0.142 ... 0.188)	-0.12 (-0.29 ... 0.031)	32.3
EC-Earth3P HighResMIP (1)	good	reasonable	0.108 (0.0910 ... 0.121)	-0.30 (-0.43 ... -0.16)	19.7
CNRM-CM6-1 HighResMIP (1)	reasonable	bad	0.187 (0.150 ... 0.219)	0.16 (-0.023 ... 0.32)	32.7
CMCC-CM2-HR4 HighResMIP (1)	good	bad	0.218 (0.177 ... 0.249)	-0.022 (-0.15 ... 0.11)	32.1
MPI-ESM1-2-HR HighResMIP (1)	good	good	0.143 (0.116 ... 0.166)	-0.10 (-0.22 ... 0.025)	19.4

GFDL-CM2.5 / FLOR historical-rcp45 (5)	good	good	0.164 (0.150 ... 0.175)	0.016 (-0.049 ... 0.083)	27.7
CCLM4 / CNRM-CM5 Cordex (r1)	good	good	0.161 (0.121 ... 0.193)	-0.14 (-0.33 ... 0.063)	34.4
CCLM4 / EC-EARTH Cordex (r12)	good	good	0.155 (0.116 ... 0.182)	-0.25 (-0.43 ... -0.013)	29.5
CCLM4 / HadGEM2-ES Cordex (r1)	reasonable	good	0.167 (0.132 ... 0.197)	-0.063 (-0.34 ... 0.087)	37.0
CCLM4 / MPI--ESM-LR Cordex (r1)	reasonable	good	0.170 (0.131 ... 0.200)	-0.097 (-0.28 ... 0.11)	39.3
HIRHAM5 / EC-EARTH Cordex (r1)	good	good	0.180 (0.142 ... 0.210)	-0.053 (-0.23 ... 0.14)	29.4
REMO20009 / IPSL-CM5A-LR Cordex (r3)	good	bad	0.154 (0.120 ... 0.180)	-0.11 (-0.29 ... 0.070)	46.1
REMO20009 / MIROC5 Cordex (r1)	good	good	0.202 (0.152 ... 0.235)	-0.096 (-0.28 ... 0.19)	36.7
REMO20009 / HadGEM2-ES Cordex (r1)	good	bad	0.179 (0.145 ... 0.206)	-0.011 (-0.20 ... -0.20)	44.6
RACMO22T / EC-EARTH Cordex (r1)	good	good	0.208 (0.171 ... 0.237)	-0.15 (-0.37 ... 0.082)	26.1
RACMO22T / HadGEM2-ES Cordex (r1)	reasonable	good	0.213 (0.171 ... 0.249)	0.12 (-0.27 ... 0.39)	31.9
RCA4 / CanESM2 Cordex (r1)	good	good	0.202 (0.166 ... 0.230)	-0.11 (-0.36 ... 0.069)	41.6
RCA4 / CNRM-CM5 Cordex (r1)	reasonable	bad	0.183 (0.149 ... 0.208)	-0.19 (-0.33 ... -0.082)	42.2
RCA4 / CSIRO-Mk3 Cordex (r1)	good	good	0.238 (0.181 ... 0.278)	-0.16 (-0.35 ... 0.094)	43.9
RCA4 / EC-EARTH Cordex (r1)	good	bad	0.164 (0.131 ... 0.190)	-0.10 (-0.30 ... 0.091)	38.2
RCA4 / EC-EARTH Cordex (r3)	good	bad	0.155 (0.124 ... 0.177)	-0.0050 (-0.25 ... 0.19)	38.4

RCA4 / EC-EARTH Cordex (r12)	good	bad	0.168 (0.137 ... 0.196)	-0.13 (-0.33 ... 0.058)	38.6
RCA4 / IPSL-CM5A-LR Cordex (r1)	reasonable	bad	0.198 (0.161 ... 0.229)	-0.31 (-0.55 ... -0.054)	49.0
RCA4 / MIROC5 Cordex (r1)	good	good	0.204 (0.168 ... 0.235)	-0.12 (-0.33 ... 0.062)	37.3
RCA4 / HadGEM2-ES Cordex (r1)	reasonable	bad	0.209 (0.172 ... 0.237)	-0.32 (-0.56 ... 0.12)	37.6
RCA4 / MPI-ESM-LR Cordex (r1)	reasonable	good	0.193 (0.158 ... 0.222)	-0.093 (-0.24 ... 0.024)	46.0
RCA4 / MPI-ESM-LR Cordex (r2)	reasonable	good	0.180 (0.149 ... 0.207)	-0.17 (-0.38 ... -0.025)	41.4
RCA4 / MPI-ESM-LR Cordex (r3)	reasonable	good	0.202 (0.170 ... 0.229)	-0.11 (-0.32 ... 0.016)	45.1
RCA4 / NorESM1 Cordex (r1)	good	good	0.191 (0.154 ... 0.216)	-0.11 (-0.32 ... 0.049)	46.7

Table2. *Evaluation results for the climate models considered for the attribution analysis of Tropical Storm Ana in the MM-box. The table contains qualitative assessments of seasonal cycle and spatial pattern of precipitation from the models (good, reasonable, bad) along with estimates for dispersion parameter, shape parameter and event magnitude. The corresponding estimates for observations are shown in blue. Based on overall suitability, the models are classified as good, reasonable and bad, shown by green, yellow and red highlights, respectively.*

Observations	**Seasonal cycle**	**Spatial pattern**	**Dispersion**	**Shape parameter**	**Event magnitude**
CHIRPS			0.187 (0.135 ... 0.221)	-0.21 (-0.40 ... -0.038)	20.3
TAMSAT			0.156 (0.109 ... 0.189)	0.019 (-0.15 ... 0.18)	25.7
ERA5			0.261 (0.214 ... 0.296)	0.12 (-0.088 ... 0.27)	27.1

Model					Threshold for 2-yr return period
CMCC-CM2-VHR4 HighResMIP (1)	good	reasonable	0.248 (0.192 ... 0.297)	0.30 (0.11 ... 0.46)	32.49
CNRM-CM6-1-HR HighResMIP (1)	good	good	0.415 (0.333 ... 0.469)	0.18 (-0.079 ... 0.40)	22.42
EC-Earth3P-HR HighResMIP (1)	good	good	0.210 (0.174 ... 0.241)	0.019 (-0.19 ... 0.18)	18.03
HadGEM3-GC31-HM HighResMIP (1)	good	good	0.262 (0.220 ... 0.291)	-0.17 (-0.31 ... -0.018)	38.11
MPI-ESM1-2-XR HighResMIP (1)	good	reasonable	0.103 (0.0860 ... 0.116)	-0.049 (-0.23 ... 0.084)	12.89
HadGEM3-GC31-MM HighResMIP (1)	good	reasonable	0.211 (0.175 ... 0.241)	0.093 (-0.14 ... 0.25)	26.82
EC-Earth3P HighResMIP (1)	good	good	0.131 (0.104 ... 0.156)	0.15 (-0.0070 ... 0.29)	19.86
CNRM-CM6-1 HighResMIP (1)	good	good	0.262 (0.208 ... 0.312)	0.21 (0.080 ... 0.33)	23.30
MPI-ESM1-2-HR HighResMIP (1)	good	reasonable	0.119 (0.0920 ... 0.138)	-0.019 (-0.15 ... 0.14)	12.73
CMCC-CM2-HR4	good	reasonable	0.254 (0.193 ... 0.310)	0.37 (0.20 ... 0.51)	22.57
GFDL-CM2.5 / FLOR historical-rcp45 (5)	good	good	0.231 (0.212 ... 0.248)	-0.034 (-0.11 ... 0.030)	26.71
CCLM4 / CNRM-CM5 Cordex (r1)	reasonable	good	0.223 (0.179 ... 0.259)	-0.051 (-0.37 ... 0.16)	32.57

CCLM4 / EC-EARTH Cordex (r12)	reasonable	good	0.205 (0.166 ... 0.237)	-0.16 (-0.31 ... 0.0010)	35.68
CCLM4 / HadGEM2-ES Cordex (r1)	reasonable	good	0.286 (0.235 ... 0.324)	-0.27 (-0.56 ... 0.0)	32.72
CCLM4 / MPI--ESM-LR Cordex (r1)	good	good	0.221 (0.169 ... 0.257)	-0.16 (-0.33 ... 0.036)	38.45
HIRHAM5 / EC-EARTH Cordex (r1)	bad	good	0.235 (0.194 ... 0.267)	0.026 (-0.10 ... 0.16)	24.33
REMO20009 / IPSL-CM5A-LR Cordex (r3)	good	bad	0.184 (0.143 ... 0.215)	-0.23 (-0.47 ... -0.041)	48.16
REMO20009 / MIROC5 Cordex (r1)	good	good	0.245 (0.198 ... 0.284)	-0.11 (-0.32 ... 0.031)	33.49
REMO20009 / HadGEM2-ES Cordex (r1)	reasonable	bad	0.201 (0.168 ... 0.231)	-0.14 (-0.59 ... -0.0070)	49.31
RACMO22T / EC-EARTH Cordex (r1)	bad	good	0.361 (0.298 ... 0.409)	-0.19 (-0.38 ... -0.059)	27.92
RACMO22T / HadGEM2-ES Cordex (r1)	reasonable	good	0.317 (0.263 ... 0.353)	-0.17 (-0.42 ... 0.13)	28.08
RCA4 / CanESM2 Cordex (r1)	good	good	0.180 (0.142 ... 0.212)	-0.26 (-0.51 ... -0.13)	44.59
RCA4 / CNRM-CM5 Cordex (r1)	reasonable	bad	0.183 (0.141 ... 0.211)	-0.032 (-0.22 ... 0.11)	48.87
RCA4 / CSIRO-Mk3 Cordex (r1)	good	good	0.294 (0.239 ... 0.340)	-0.33 (-0.51 ... -0.20)	36.59

RCA4 / EC-EARTH Cordex (r1)	reasonable	bad	0.161 (0.125 ... 0.192)	-0.29 (-0.54 ... -0.11)	48.32
RCA4 / EC-EARTH Cordex (r3)	reasonable	bad	0.180 (0.148 ... 0.207)	-0.14 (-0.31 ... 0.029)	44.88
RCA4 / EC-EARTH Cordex (r12)	reasonable	bad	0.160 (0.127 ... 0.184)	-0.17 (-0.39 ... -0.046)	46.18
RCA4 / IPSL-CM5A-LR Cordex (r1)	good	bad	0.133 (0.107 ... 0.151)	-0.14 (-0.32 ... 0.015)	54.03
RCA4 / MIROC5 Cordex (r1)	good	good	0.213 (0.172 ... 0.245)	-0.25 (-0.42 ... -0.092)	42.85
RCA4 / HadGEM2-ES Cordex (r1)	reasonable	bad	0.151 (0.118 ... 0.176)	-0.20 (-0.40 ... -0.024)	55.31
RCA4 / MPI-ESM-LR Cordex (r1)	good	good	0.173 (0.140 ... 0.202)	-0.40 (-0.69 ... -0.25)	50.23
RCA4 / MPI-ESM-LR Cordex (r2)	good	good	0.181 (0.147 ... 0.210)	-0.32 (-0.67 ... -0.19)	50.54
RCA4 / MPI-ESM-LR Cordex (r3)	good	good	0.147 (0.122 ... 0.165)	-0.24 (-0.46 ... -0.049)	50.30
RCA4 / NorESM1 Cordex (r1)	good	good	0.196 (0.156 ... 0.232)	-0.38 (-0.68 ... -0.12)	42.62

Table3*. Same as Table 2, for attribution analysis of Cyclone Batsirai in Madagascar.*

5 Multi-method multi-model attribution

This section shows Probability Ratios and change in rain event intensity ΔI for models and also includes the values calculated from the fits with observations. Tables 4 and 5 show only the models that are labelled "good".

Model / Observations	Threshold for return period 2 yr	Probability ratio PR [-]	Change in intensity ΔI [mm/day]
CHIRPS	20 mm/day	0.97 (0.66 ... 1.7)	-3.0 (-31 ... 35)
TAMSAT	26 mm/day	0.56 (0.10 ... 4.9)	-9.6 (-31 ... 23)
ERA5	27 mm/day	2.4 (1.1 ... 6.4)	33 (3.5 ... 76)
EC-Earth3P-HR HighResMIP (1)	18 mm/day	0.83 (0.45 ... 1.5)	-5.5 (-21 ... 17)
HadGEM3-GC31-HM HighResMIP (1)	38 mm/day	2.9 (0.79 ... 12)	26 (-4.8 ... 57)
EC-Earth3P HighResMIP (1)	20 mm/day	0.89 (0.51 ... 1.8)	-2.2 (-14 ... 11)
CNRM-CM6-1 HighResMIP (1)	23 mm/day	1.1 (0.61 ... 1.9)	2.4 (-17 ... 26)
CCLM4 / CNRM-CM5 Cordex (r1)	33 mm/day	1.5 (0.59 ... 2.8)	10 (-11 ... 31)
CCLM4 / EC-EARTH Cordex (r12)	36 mm/day	1.3 (0.58 ... 3.0)	6.8 (-11 ... 25)
CCLM4 / HadGEM2-ES Cordex (r1)	33 mm/day	1.2 (0.25 ... 2.0)	6.5 (-25 ... 28)
HIRHAM5 / EC-EARTH Cordex (r1)	24 mm/day	2.2 (1.2 ... 4.3)	21 (4.2 ... 42)
REMO20009 / HadGEM2-ES Cordex (r1)	49 mm/day	1.7 (0.62 ... 3.3)	12 (-6.9 ... 33)

Table 4. *Precipitation threshold for the 2-yr return period, Probability Ratio and change in intensity for the models that passed the validation tests, for Madagascar.*

Model / Observations	Threshold for return period 50 yr	Probability ratio PR [-]	Change in intensity ΔI [%]
CHIRPS	24.884 mm/day	15 (0.16 ... ∞)	12 (-11 ... 43)

TAMSAT	15.762 mm/day	1.8 (0.45 ... 2.1e+2)	14 (-16 ... 63)
ERA5	25.383 mm/day	14 (1.3 ... ∞)	16 (1.7 ... 33)
EC-Earth3P-HR HighResMIP (1)	25 mm/day	3.4 (0.91 ... ∞)	9.9 (-1.1 ... 23)
HadGEM3-GC31-HM HighResMIP (1)	32 mm/day	2.9 (0.58 ... ∞)	8.3 (-4.9 ... 25)
MPI-ESM1-2-XR HighResMIP (1)	18 mm/day	8.9 (1.5 ... ∞)	10 (1.9 ... 21)
GFDL-CM2.5 / FLOR historical-rcp45 (5)	28 mm/day	1.9 (1.3 ... 3.0)	6.2 (2.7 ... 10)
CCLM4 / CNRM-CM5 Cordex (r1)	34 mm/day	2.8 (0.16 ... ∞)	6.0 (-7.2 ... 20)
CCLM4 / EC-EARTH Cordex (r12)	30 mm/day	0.31 (0.0031 ... ∞)	-5.9 (-18 ... 6.6)
CCLM4 / HadGEM2-ES Cordex (r1)	37 mm/day	3.6 (0.83 ... ∞)	10 (-1.6 ... 30)
CCLM4 / MPI--ESM-LR Cordex (r1)	39 mm/day	3.4 (0.50 ... 1.8e+10)	8.7 (-3.2 ... 21)
HIRHAM5 / EC-EARTH Cordex (r1)	29 mm/day	1.5 (0.26 ... 29)	-3.6 (-15 ... 11)
REMO20009 / IPSL-CM5A-LR Cordex (r3)	46 mm/day	18 (2.4 ... ∞)	16 (6.0 ... 27)
RCA4 / MPI-ESM-LR Cordex (r3)	45 mm/day	2.2 (0.14 ... ∞)	6.2 (-8.7 ... 22)

Table 5. *Same as Table 4, for the MM-box. Here, thresholds are shown for the 50-yr return period.*

6 Hazard synthesis

For each of the two event definitions we calculate the probability ratio as well as the change in magnitude of the event in the observations and the models. If the models do not pass the validation tests we do not use the results. We synthesise the ones that pass along with the observations, to give an overarching attribution statement. Observations and models are combined into a single result in two ways if they seem to be compatible. Firstly, we neglect common model uncertainties beyond the model spread that is depicted by the model average, and compute the weighted average of models and observations: this is indicated by the magenta bar. As, due to common model uncertainties, model uncertainty can be larger than the model

spread, secondly, we also show the more conservative estimate of an unweighted average of observations and models, indicated by the white box around the magenta bar in the synthesis figures.

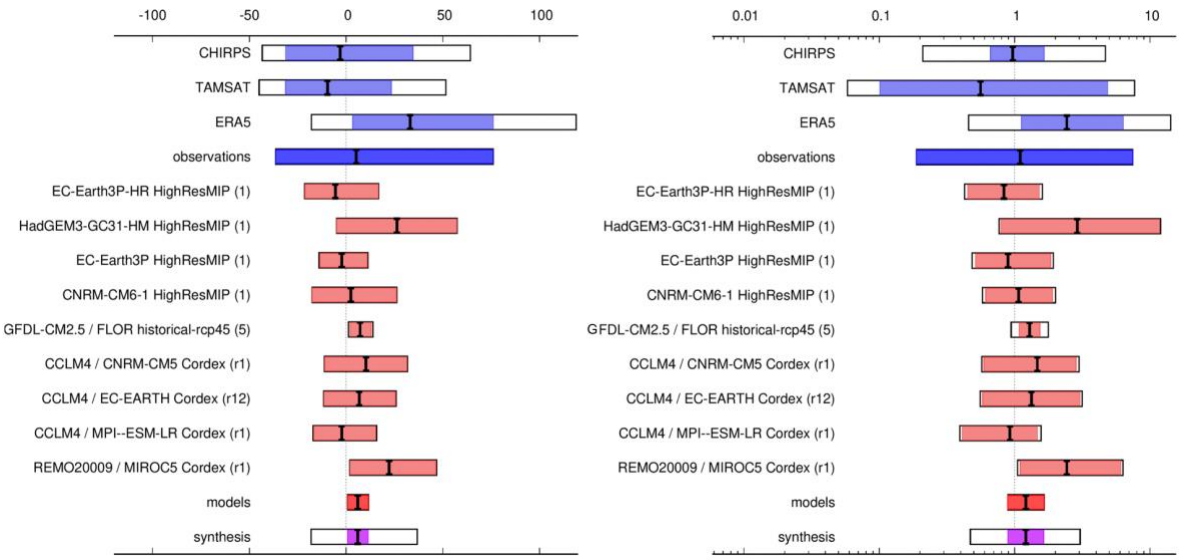

Fig11*. Synthesis of intensity change (left) and probability ratios (right), when comparing the 2-year heavy rainfall event over Madagascar with a 1.2C cooler climate.*

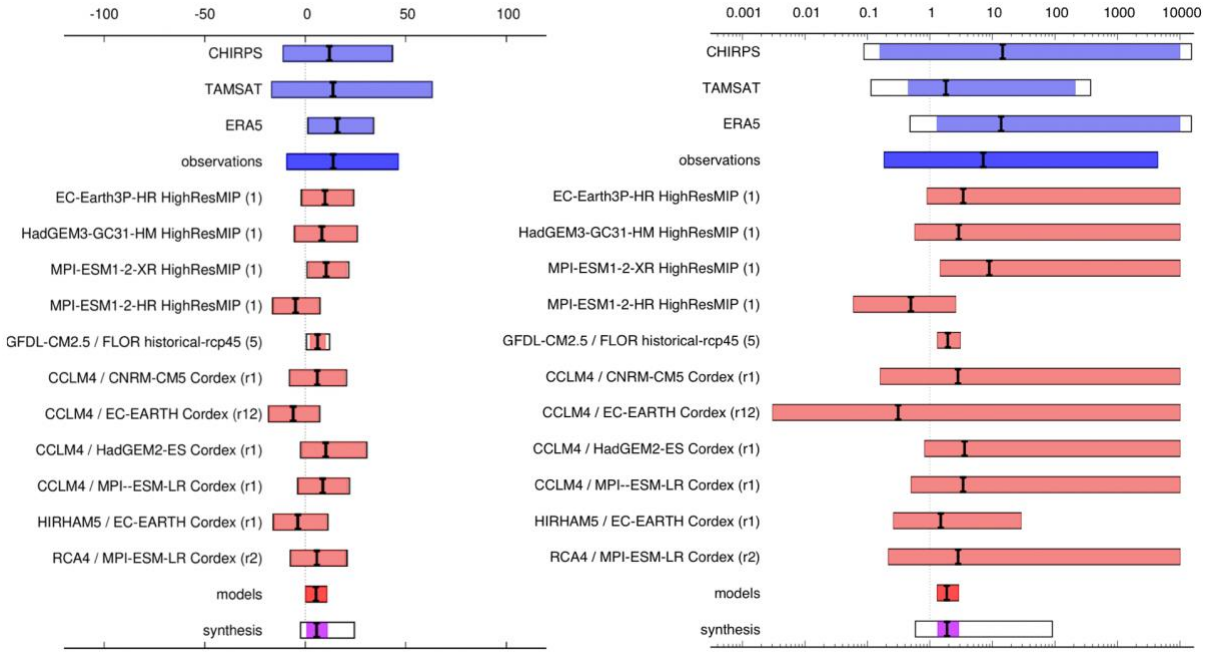

Fig12*. Synthesis of intensity change (left) and probability ratios (right), when comparing the 50-year heavy rainfall event over the Mozambique Malawi region with a 1.2C cooler climate.*

The evaluation of models in this study has proven difficult due to the very large discrepancies in the observational data. For both event definitions the parameters of the GEV distribution span a very large range, thus providing only loose criteria to exclude models. For the synthesis we thus concentrated on models that showed a good representation of the observed rainfall patterns as well as the seasonal cycle and excluded all models whose parameters were outside the (still large) range of the best estimates for the observed parameters. The overarching results are however not sensitive to whether the models with parameters labelled as “reasonable” are

included in the synthesis. Figures 11 & 12 show the synthesis only including the models having passed the stricter evaluation criteria.

For both events the synthesis shows an increase in the intensity and probability ratios where the increase in intensity is of the order expected from the Clausius-Clapeyron relationship and probability ratios indicate very roughly a doubling in likelihood. The uncertainty around this result is so large, that exact values are not informative. In fact, given the large discrepancy in trends in models as well as observations, a quantitative synthesis is only reported here for illustration, the quality of the observations and subsequent inability to identify fit-for-purpose models renders any quantitative assessment meaningless as well as the notion of statistical significance. Qualitatively however, it is important to highlight that with small sensitivity to the exact choice of models that there is an increase in intensity and likelihood, suggesting that heavy rain as observed in the regions in 2022 is a harbinger of what is to come.

This finding is in line with global research on tropical cyclones, e.g. summarised by Knutson et al. (2020) highlighting that precipitation rates associated with tropical cyclones will rise with further warming.

7 Vulnerability and exposure

What turns a hazard into a humanitarian disaster is generally understood as a combination of exposure and vulnerability (including coping capacity) which combined make a community or household better or worse equipped to respond to hazard risk and lessen its impact.

INFORM Risk Index

The INFORM index, a collaboration of the Inter-Agency Standing Committee Reference Group on Risk, Early Warning and Preparedness and the European Commission, is a framework to quantify the level of humanitarian risk in a country, based on the three dimensions of risk: hazard exposure, vulnerability, and coping capacity. Through 54 different indicators, it builds a risk score out of 10 for each country (INFORM Risk Methodology, 2017). INFORM ranks disaster risk in Mozambique as “very high”, notably due to medium exposure to cyclones and floods, high vulnerability (7.6/10) notably due to high inequality, rates of displacement, and socio-economic conditions, and a low coping capacity (6.3/10). The same index ranks risk in Malawi as “medium” notably due to medium exposure to floods (5.3/10) , medium vulnerability and medium-low lack of coping capacity (6.4/10) notably due to vulnerable infrastructure and warning communication. Finally, risk in Madagascar is ranked as “high”, product of a high exposure to cyclones and floods, medium vulnerability (5/10) linked to “low development” and “deprivation” (8.7/10) and presence of vulnerable groups including marginalised indigenous populations, and high lack of coping capacity (7/10) notably due to highly exposed and vulnerable infrastructure and limited warning communication structure (INFORM 2022).

Among the many vulnerability and exposure dynamics which are being uncovered in post-disaster reporting and research on storm Ana and cyclone Batsirai, common themes across both events and the three countries include the presence of compound events, varying levels of warning and preparedness, and a range of socio-economic impacts which made certain populations particularly vulnerable to the storms.

a. Forecasts, warning, and preparedness

Warning and preparedness are a key tool to reduce the impact of disasters. The Southern Africa region sees multiple tropical storms and cyclones per year and has developed robust forecasting, warning, and preparedness to these hazards. For instance, Madagascar's cyclone and flooding contingency plan is updated every year and includes elements such as, plans for different cyclone scenarios, budgets for preposition, and warning communication networks (Repoblikan'i Madagasikara, 2013) - the latest was updated in November 2021 (Actu Orange, 2021). Similarly, Mozambique experiences at least one tropical cyclone landfall a year, on average (1958-2008) (Bettinger and Merry, 2012). Tropical disturbances, storms, and cyclones in the Southern Indian Ocean are relatively well-tracked and understood, monitored by a range of institutions such as Météo Madagascar, South Africa Weather Services (SAWS), Instituto Nacional de Meteorologia de Moçambique (INAM), and the Direction of Météo-France in La Réunion, a designated Regional Specialised Meteorological Centre (RSMC) responsible for the monitoring of all the tropical systems occurring over South-West Indian Ocean.

Both tropical storm Ana and cyclone Batsirai were well forecasted and tracked, notably by Météo Madagascar and the Regional Specialised Meteorological Centre. A track of cyclone Ana was first communicated on January 16th by MétéoFrance / Piroi and INAM warning bulletins 8 days before it made landfall in Mozambique. Ana moved rapidly through Madagascar to the Mozambique channel within 24 hours, rapidly intensifying and hitting Angoche District in Nampula Province on January 24th (OCHA, 2022c). Cyclone Batsirai was identified approximately with a 9 days lead-time. (MétéoFrance, 2022). The flooding caused by the storms was also the subject of warnings in all three countries. For example, on the 21st January, the National Directorate for Water Resources Management (DNGRH) in Mozambique issued warnings for increasing levels in the river basins of Zambeze (Sub basins of Revubue e Chire), Licungo, coastal basins of the Zambezia, Nampula and Cabo Delgado provinces and a risk of moderate to high urban flooding for the cities of Beira and Quelimane and erosion risk for the city of Nacala Porto (DNGRH, 2022).

However, the existence of warnings does not guarantee that these warnings are received and acted upon. Notably, the general damage to communication structures and electrical grids may have hampered the reception of the warnings; and lead times of the warning may have influenced the level of greater warning-based actions. Additionally, lack of trust in the forecast information has also been reported as hindering the effectiveness of the warnings (IFRC, 2022c). Deeper investigation and analysis would be required to understand the role these elements played in enhancing or limiting impacts.

b. Compound events

In the climate hazard literature, compound events are defined as the overlap of multiple hazards and/or drivers that combine to increase social or environmental risk (Zscheischler et al., 2018; Zscheischler et al., 2020; Raymond et al., 2020). This can includes a variety of combinations: (1) more than one extreme event happening at the same time or not long after one another, (2) different combinations of extreme events over underlying vulnerable conditions, (3) or the occurrence of multiple events which on their own cannot be considered extreme but their impacts are (IPCC, 2012 (SREX); Cato and Dowdy, 2021).

All three of these definitions apply to storm Ana and cyclone Batsirai, both which hit with high rainfall intensity in river catchments that were already in the midst of a particularly rainy season (IFRC, 2022d). Indeed, both Malawi and Mozambique had experienced flooding

in the weeks preceding Ana, and the communities affected by those floods were left particularly vulnerable to additional hazards, in particular one that compounded the existing flood situations - consecutive tropical storms do not allow people to recover before another one hits. Underlying conditions of conflict (northern Mozambique), drought (southern Madagascar) may also be important to explore further. Notably, Madagascar is currently grappling with an extreme food insecurity situation, driven by a range of socio-economic conditions and a prolonged drought (see Harrington *et al.*, 2021). Although the track of cyclone Batsirai itself did not pass through the regions most affected by the drought, the national and humanitarian capacity for disaster response in the country is stretched thin from this prolonged crisis.

c. Socio-economic context

Related to the concept of compound events, socio-economic contexts of the impact region can help to understand the differential impacts of both storms. Generally speaking, certain people are at greater risk of dying or being injured during rapid-onset events, for example, elderly people, people with disabilities, and children (IDMC, n.d.). At the same time, poorer, marginalised, and displaced communities are more likely to live in at-risk areas such as floodplains, making them more exposed to certain events (Adger et al., 2018; Thalheimer et al., 2022). Marginalised people or communities are also less likely to receive early warnings or be reached during disasters and often have limited resources to cope (Behlert *et al.*, 2020). In Mozambique, much of the affected communities' experienced reduced resilience and a limited ability to rebuild their homes after having been impacted by recurring storms, namely by 2019 cyclones Idai and Kenneth, and 2021 tropical storm Eloise (IFRC, 2022e). In Madagascar, socio-economic conditions are particularly low in rural areas which fare much worse on child mortality, school attendance, literacy and primary school completion rates, malnutrition, life expectancy, access to transport, electricity, potable water (World Bank, 2020). In Malawi, the areas of highest impact from storm Ana also seem to correspond to poverty incidence (IFPRI, 2017).

Finally, the damage to livelihoods and assets caused by Ana and Bastirai are also determined by their exposure to the flooding brought by the storm. For context, the region's economy is dominated by the agricultural sector which employs 64% of the workforce in Madagascar (World Bank, 2021a), 70% in Mozambique (World Bank, 2021b), and 76% in Malawi (World Bank, 2021c). Much of these agricultural lands are located in the floodplains of the impacted region, where land is particularly fertile. Floodplains account for the high damages to the three countries' economies. Prior to the event, these lands had already been impacted by a strong rainy season, and crops were further damaged by the storm. In addition, the Covid-19 pandemic has had significant impacts on the region's economic situation, as highlighted in V&E section of the 2021 Madagascar drought attribution study (see Harrington et al., 2021). For Madagascar, the pandemic has reversed over a decade of gains in income per capita and poverty reduction - export-oriented sector (mainly agricultural) have been most impacted and domestic-oriented sectors dragged down by declining income (World Bank, 2020) - over 2 million people have already fallen below the international poverty line of $1.90/capita (OCHA, 2022a). In Malawi, 91,000 households and approximately 71,000 hectares of crops were critically impacted. Around 12,655 livestock keepers, including 37,000 livestock were injured or killed (OCHA, 2022b). Conversely, the flooding exacerbated the hardest-hit regions' food insecurity, which were already forecast to reach acute levels in March 2022 (Ibid.).

Vulnerability and Exposure Conclusion

The devastating impact of these storms, and the attribution of the heavy rainfall to climate change, once again confirms that climate change is already impacting the most vulnerable countries and communities. Climate change is elevating risk in places where tropical cyclones are already affecting agriculture, infrastructure, livelihoods and lives. The compounding of multiple rainfall events makes it more difficult for communities to recover and prepare for the next event. Reconstruction efforts will need to account for increased risk of rainfall related impacts, as well as the possibility of compounding crises, when making decisions about rebuilding infrastructure and strengthening early warning systems. Similarly ongoing development investments in this region need to incorporate rising risks across hazards and sectors to reduce future impacts and avoid locking in future risks. Reducing climate risks in this region will require both mitigation efforts from emitters around the world, as well as, inclusive, locally led adaptation. Future research into vulnerability and exposure dynamics, as well as robust recommendations for risk reduction will strengthen resilience building efforts.

Data availability

All data that are used for the synthesis are available via the Climate Explorer at https://climexp.knmi.nl/MMM2022.cgi.

References

Actu Orange. 2021. “Réponses aux cyclones et inondations, un budget non couvert de 28,9 millions de dollar américain par rapport aux stocks d’urgence, selon le BNGRC”. Actu Orange. https://actu.orange.mg/cyclones-et-inondations-un-budget-non-couvert-de-289-millions-de-dollars-americains-par-rapport-aux-stocks-durgence-selon-le-bngrc/

Adger, W. N., de Campos, R. S., & Mortreux, C. (2018). Mobility, displacement and migration, and their interactions with vulnerability and adaptation to environmental risks. In Routledge handbook of environmental displacement and migration (pp. 29-41). Routledge.

Al Jazeera. 7 February 2022. “Cyclone Batsirai: At least 20 killed in Madagascar tropical storm.” Al Jazeera. https://www.aljazeera.com/news/2022/2/7/cyclone-kills-20-in-madagascar-but-quickly-weakens-on-land

Behlert et al., 2020. World Risk Report 2020. https://reliefweb.int/sites/reliefweb.int/files/resources/WorldRiskReport-2020.pdf

Bettinger, P. and Merry, K.L., 2012. Relative vulnerability of the forests along southeastern African coasts to cyclones. Singapore journal of tropical geography, 33(3), pp.320-334.

Burns, J. M., Subrahmanyam, B., Nyadjro, E. S., & Murty, V. S. N. (2016). Tropical cyclone activity over the southwest tropical Indian Ocean. *Journal of Geophysical Research: Oceans*, *121*(8), 6389-6402.

Camberlin, P., Janicot, S., & Poccard, I. (2001). Seasonality and atmospheric dynamics of the teleconnection between African rainfall and tropical sea-surface temperature: Atlantic vs. ENSO. *International Journal of Climatology: A Journal of the Royal Meteorological Society*, *21*(8), 973-1005.

CARE. 2022.” CYCLONE BATSIRAI: Initial Assessments Paint A Grim Picture As Another Cyclone Forms”. https://www.care.org/news-and-stories/press-releases/cyclone-batsirai-initial-assessments-paint-a-grim-picture-as-another-cyclone-forms/

Catto, J.L. and Dowdy, A., 2021. Understanding compound hazards from a weather system perspective. Weather and Climate Extremes, 32, p.100313.

Cattiaux, J., Chauvin, F., Bousquet, O., Malardel, S., & Tsai, C. L. (2020). Projected changes in the Southern Indian Ocean cyclone activity assessed from high-resolution experiments and CMIP5 models. *Journal of Climate*, *33*(12), 4975-4991.

Ciavarella, A., Cotterill, D., Stott, P., Kew, S., Philip, S., van Oldenborgh, G. J., et al. (2021). Prolonged Siberian heat of 2020 almost impossible without human influence. *Climatic Change*, *166* (1), 9. https://doi.org/10.1007/s10584-021-03052-w

DNGRH, 2021, Boletim Hidrológico Nacional, Edição Nº17. 21/01/2021, MINISTÉRIO DAS OBRAS PÚBLICAS, HABITAÇÃO E RECURSOS HÍDRICOS, Departamento de Gestão de Bacias Hidrográficas. https://drive.google.com/file/d/12dwndnO2rHWwIrOo4nueskpEi5H31GXC/view

Ebi, K. L., Teisberg, T. J., Kalkstein, L. S., Robinson, L., & Weiher, R. F. (2004). Heat Watch/ Warning Systems Save Lives: Estimated Costs and Benefits for Philadelphia 1995–98. Bulletin of the American Meteorological Society, 85(8), 1067-1074, doi:10.1175/bams-85-8-1067.

ECHO. 2022. "Madagascar - Tropical Cyclone BATSIRAI, update (BNGRC, Meteo Madagascar) (ECHO Daily Flash of 11 February 2022)". https://reliefweb.int/report/madagascar/madagascar-tropical-cyclone-batsirai-update-bngrc-meteo-madagascar-echo-daily

Emanuel, K. (2017). Assessing the present and future probability of Hurricane Harvey's rainfall. *Proceedings of the National Academy of Sciences*, *114*(48), 12681-12684.

Famine Early Warning System (FEWSNet). https://fews.net/

France 24. 29 January 2022. "Tropical Storm Ana leaves trail of destruction in Madagascar".

Fouillet, A., Rey, G., Wagner, V., Laaidi, K., Empereur-Bissonnet, P., Le Tertre, A., ... & Jougla, E. (2008). Has the impact of heat waves on mortality changed in France since the European heat wave of summer 2003? A study of the 2006 heat wave. International journal of epidemiology, 37(2), 309-317.

Funk, C., Peterson, P., Landsfeld, M., Pedreros, D., Verdin, J., Shukla, S., et al. (2015). The climate hazards infrared precipitation with stations—a new environmental record for monitoring extremes. *Scientific Data*, *2*(1), 150066. https://doi.org/10.1038/sdata.2015.66

GDACS. 2022. "Overall Orange alert Tropical Cyclone for ANA-22." https://www.gdacs.org/report.aspx?eventid=1000858&episodeid=3&eventtype=TC

Gerretsen, I. February 1, 2022. "Storm Ana's devastation in southern Africa highlights need for early warnings". Climate Home News. https://www.climatechangenews.com/2022/02/01/storm-anas-devastation-southern-africa-highlights-need-early-warnings/

Gleixner, S., Demissie, T., & Diro, G. T. (2020). Did ERA5 improve temperature and precipitation reanalysis over East Africa?. *Atmosphere*, *11*(9), 996.

Hansen, J., Ruedy, R., Sato, M., and Lo, K. (2010). Global surface temperature change. Rev. Geophys., 48, RG4004, doi:10.1029/2010RG000345.

Harrington et al. 2021. "Attribution of severe low rainfall in southern Madagascar, 2019-21". World Weather Attribution. https://www.worldweatherattribution.org/wp-content/uploads/ScientificReport_Madagascar.pdf

https://reliefweb.int/report/madagascar/southern-africa-cyclone-season-flash-update-no-6-tropical-cyclone-batsirai-13

Hart, N. C. G., Washington, R., and Reason, C. J. C. (2018). On the Likelihood of Tropical–Extratropical Cloud Bands in the South Indian Convergence Zone during ENSO Events. *J. Clim.* 31, 2797–2817. doi:10.1175/JCLI-D-17-0221.1.

Hersbach, H., Bell, B., Berrisford, P., Hirahara, S., Horányi, A., Muñoz-Sabater, J., et al. (2020). The ERA5 global reanalysis. *Quarterly Journal of the Royal Meteorological Society*, *146*(730), 1999–2049. https://doi.org/10.1002/qj.3803

Hoell, A., Funk, C., Magadzire, T., Zinke, J., and Husak, G. (2015). El Niño–Southern Oscillation diversity and Southern Africa teleconnections during Austral Summer. *Clim. Dyn.* 45, 1583–1599. doi:10.1007/s00382-014-2414-z.

IDMC. n.d. "Disasters and Climate Change". Internal Displacement Monitoring Centre. https://www.internal-displacement.org/disasters-and-climate-change

IFPRI. 2017. "Poverty in Malawi 2016–2017". International Food Policy Research Institute. https://massp.ifpri.info/files/2019/06/Poster-on-Poverty-in-Malawi-2016-2017.pdf

IFRC. 2022d. "OPERATIONAL STRATEGY Malawi, Africa | Tropical Storm Ana". https://reliefweb.int/sites/reliefweb.int/files/resources/MDRMW015OU1.pdf

IFRC. 2022a. "Malawi, Africa | Tropical Storm Ana - Emergency Appeal N°: MDRMW015". https://reliefweb.int/report/malawi/malawi-africa-tropical-storm-ana-emergency-appeal-n-mdrmw015-operational-strategy-24

IFRC. 2022b. "Malawi - Tropical Storm Ana (MDRMW015)." https://www.ifrc.org/media/50257

IFRC. 2022e. "REVISED EMERGENCY APPEAL Mozambique, Africa | 2021-22 Floods and Cyclones". https://reliefweb.int/sites/reliefweb.int/files/resources/MDRMZ016rea1.pdf

INFORM. 2017. "INFORM Risk Index Methodology". https://drmkc.jrc.ec.europa.eu/inform-index

INFORM. 2022. "Country Risk Profile". https://drmkc.jrc.ec.europa.eu/inform-index/INFORM-Risk/Country-Risk-Profile

IPCC, 2012 – Field, C.B., V. Barros, T.F. Stocker, D. Qin, D.J. Dokken, K.L. Ebi, M.D. Mastrandrea, K.J. Mach, G.-K. Plattner, S.K. Allen, M. Tignor, and P.M. Midgley (Eds.) Available from Cambridge University Press,

Kossin, J. P., Knapp, K. R., Olander, T. L., & Velden, C. S. (2020). Global increase in major tropical cyclone exceedance probability over the past four decades. *Proceedings of the National Academy of Sciences*, *117*(22), 11975-11980.

Kovats, S. and Hajat, S. (2008), Heat Stress and Public Health: A Critical Review. Annual Review Public Health 29, 41-55, doi: 10.1146/annurev.publhealth.29.020907.090843.

Knutson, T., Camargo, S. J., Chan, J. C., Emanuel, K., Ho, C. H., Kossin, J., ... & Wu, L. (2020). Tropical cyclones and climate change assessment: Part II: Projected response to anthropogenic warming. *Bulletin of the American Meteorological Society*, *101*(3), E303-E322.

Knutson, T. R., Sirutis, J. J., Zhao, M., Tuleya, R. E., Bender, M., Vecchi, G. A., ... & Chavas, D. (2015). Global projections of intense tropical cyclone activity for the late twenty-first century from dynamical downscaling of CMIP5/RCP4. 5 scenarios. *Journal of Climate*, *28*(18), 7203-7224.

Lenssen, N., Schmidt, G., Hansen, J., Menne, M., Persin, A., Ruedy, R., and Zyss, D. (2019). Improvements in the GISTEMP uncertainty model. J. Geophys. Res. Atmos., 124(12), 6307-6326, doi:10.1029/2018JD029522.

Luu, L. N., Scussolini, P., Kew, S., Philip, S., Hariadi, M. H., Vautard, R., ... & Van Oldenborgh, G. J. (2021). Attribution of typhoon-induced torrential precipitation in Central Vietnam, October 2020. *Climatic Change*, *169*(3), 1-22.

Maidment, R., Grimes, D., Allan, R., Tarnavsky, E., Stringer, M., Hewison, T., Roebeling, R., and Black, E. (2014). The 30-year TAMSAT African Rainfall Climatology and Time-series (TARCAT) Data Set. *Journal of Geophysical Research: Atmospheres*, 119(10): 619-610, 644. DOI: 10.1002/2014JD021927.

Maidment, R. I., D. Grimes, E. Black, E. Tarnavsky, M. Young, H. Greatrex, R. P. Allan et al. (2017). A new, long-term daily satellite-based rainfall dataset for operational monitoring in Africa. *Nature Scientific Data*, 4: 170063. DOI: 10.1038/sdata.2017.63.

MapAction. 2022. "Madagascar: Tropical Cyclone Batsirai". https://reliefweb.int/map/madagascar/madagascar-tropical-cyclone-batsirai-cumulative-rainfall-1st-7th-february-2022-0

Mavume, A. F., Rydberg, L., Rouault, M., & Lutjeharms, J. R. (2009). Climatology and landfall of tropical cyclones in the south-west Indian Ocean. *Western Indian Ocean Journal of Marine Science*, *8*(1).

MSF. 2022. "Cyclone Batsirai leaves people vulnerable to food shortages and malaria". Médecins Sans Frontières. https://reliefweb.int/report/madagascar/cyclone-batsirai-leaves-people-vulnerable-food-shortages-and-malaria

Muthige, M. S., Malherbe, J., Englebrecht, F. A., Grab, S., Beraki, A., Maisha, T. R., & Van der Merwe, J. (2018). Projected changes in tropical cyclones over the South West Indian Ocean under different extents of global warming. *Environmental Research Letters*, *13*(6), 065019.

Nikulin, G., Jones, C., Giorgi, F., Asrar, G., Büchner, M., Cerezo-Mota, R., Christensen, O. B., Déqué, M., Fernandez, J., Hänsler, A., van Meijgaard, E., Samuelsson, P., Sylla, M. B., & Sushama, L. (2012). Precipitation Climatology in an Ensemble of CORDEX-Africa Regional Climate Simulations, *Journal of Climate*, *25*(18), 6057-6078. Retrieved Apr 8, 2022, from https://journals.ametsoc.org/view/journals/clim/25/18/jcli-d-11-00375.1.xml

OCHA. 2022a. Mozambique - Tropical Storm Ana - Flash Update No. 7. https://reliefweb.int/sites/reliefweb.int/files/resources/FlashUpdate%237_DRAFT_20220201_MOZ.pdf

OCHA. 2022b "Flash Appeal Malawi". https://reliefweb.int/sites/reliefweb.int/files/resources/ROSEA_20220224_Malawi_TropicalStorm_Ana_Flash_Appeal_Feb-Apr-2022_final.pdf

OCHA. 2022c."MOZAMBIQUE – TROPICAL STORM ANA Flash Update No.1". https://reliefweb.int/sites/reliefweb.int/files/resources/20220124_MOZ_FlashUpdate%231.pdf

OCHA. 2022d. "SOUTHERN AFRICA: Cyclone Season Flash Update No. 2". https://reliefweb.int/sites/reliefweb.int/files/resources/ROSEA_20220204_Southern%20Africa%20-%20Cyclone%20Season_Flash%20Update%20_2.pdf

OCHA. 2022e. "Southern Africa: Cyclone Season Flash Update No. 6 (Tropical Cyclone Batsirai) (13 February 2022)". https://reliefweb.int/report/madagascar/southern-africa-cyclone-season-flash-update-no-6-tropical-cyclone-batsirai-13

Patricola, C.M., Wehner, M.F. Anthropogenic influences on major tropical cyclone events. *Nature* **563,** 339–346 (2018). https://doi.org/10.1038/s41586-018-0673-2

Philip, S., Kew, S., van Oldenborgh, G. J., Otto, F., Vautard, R., van der Wiel, K., et al. (2020). A protocol for probabilistic extreme event attribution analyses. *Advances in Statistical Climatology*,

Rabary, L. 11 February 2022. "Death toll from Cyclone Batsirai in Madagascar rises to 120 - state agency". Reuters.

Raymond, C., Horton, R.M., Zscheischler, J., Martius, O., AghaKouchak, A., Balch, J., Bowen, S.G., Camargo, S.J., Hess, J., Kornhuber, K. and Oppenheimer, M., 2020. Understanding and managing connected extreme events. Nature climate change, 10(7), pp.611-621.

Repoblikan'i Madagasikara. 2013. Plan de Contingence National Cyclones et Inondations. https://www.humanitarianlibrary.org/sites/default/files/2013/07/Madagascar_plan_de_contingence_National_2012-13.pdf

Risser, M. D., & Wehner, M. F. (2017). Attributable human-induced changes in the likelihood and magnitude of the observed extreme precipitation during Hurricane Harvey. *Geophysical Research Letters*, *44*(24), 12-457.

Schneider, T., Bischoff, T., & Haug, G. H. (2014). Migrations and dynamics of the intertropical convergence zone. *Nature*, *513*(7516), 45-53.

Seneviratne, S.I., Zhang, X., et al., (2021). Weather and Climate Extreme Events in a Changing Climate., in: Masson-Delmotte, V., Zhai, P. et al. (Eds.), Climate Change 2021: The Physical Science Climate, Contribution of Working Group I to the Sixth Assessment Report of the Intergovernmental Panel on Change. Cambridge University Press.

Tarnavsky, E., Grimes, D., Maidment, R., Black, E., Allan, R., Stringer, M., Chadwick, R. and Kayitakire, F., (2014). Extension of the TAMSAT Satellite-based Rainfall Monitoring over Africa and from 1983 to present. *Journal of Applied Meteorology and Climatology*, 53(12): 2805-2822. DOI: 10.1175/JAMC-D-14-0016.1.

Thalheimer, L., Simperingham, E., & Jjemba, E. W. (2022). The role of anticipatory humanitarian action to reduce disaster displacement. Environmental Research Letters, 17(1), 014043.

Terblanche, D., Lynch, A., Chen, Z., & Sinclair, S. (2021). ERA5 derived precipitation: Insights from historical rainfall networks in southern Africa. *Journal of Applied Meteorology and Climatology*.

UNICEF. 2022. "Tropical Storm Ana wreaks havoc for children in Madagascar, Malawi, Mozambique and Zimbabwe, warns UNICEF". https://www.unicef.org/press-releases/tropical-storm-ana-wreaks-havoc-children-madagascar-malawi-mozambique-and-zimbabwe

Van Oldenborgh, G. J., Van Der Wiel, K., Sebastian, A., Singh, R., Arrighi, J., Otto, F., ... & Cullen, H. (2017). Attribution of extreme rainfall from Hurricane Harvey, August 2017. *Environmental Research Letters*, *12*(12), 124009.

van Oldenborgh, G. J., van der Wiel, K., Kew, S., Philip, S., Otto, F., Vautard, R., et al. (2021). Pathways and pitfalls in extreme event attribution. *Climatic Change*, *166* (1), 13. https://doi.org/10.1007/s10584-021-03071-7.

van Oldenborgh, G. J., Van Der Wiel, K., Sebastian, A., Singh, R., Arrighi, J., Otto, F., ... & Cullen, H. (2017). Attribution of extreme rainfall from Hurricane Harvey, August 2017. *Environmental Research Letters*, *12*(12), 124009.

WHO. 2022. "Malawi declares polio outbreak". https://reliefweb.int/report/malawi/malawi-declares-polio-outbreak

Windsor, M. 28 January 2022. "Tropical Storm Ana leaves dozens dead in southern Africa". ABC News. https://abcnews.go.com/International/tropical-storm-ana-leaves-dozens-dead-southern-africa/story?id=82531150

World Bank. 2020. "The World Bank in Madagascar - Overview". https://www.worldbank.org/en/country/madagascar/overview#1

World Bank. 2021a. "Employment in Agriculture (% of total employment) (modeled ILO estimate) Madagascar". https://data.worldbank.org/indicator/SL.AGR.EMPL.ZS?locations=MG

World Bank. 2021b. "Employment in Agriculture (% of total employment) (modeled ILO estimate) Mozambique". https://data.worldbank.org/indicator/SL.AGR.EMPL.ZS?locations=MZ

World Bank. 2021b. “Employment in Agriculture (% of total employment) (modeled ILO estimate) Malawi”. https://data.worldbank.org/indicator/SL.AGR.EMPL.ZS?locations=MW

Zscheischler, J., Martius, O., Westra, S., Bevacqua, E., Raymond, C., Horton, R.M., van den Hurk, B., AghaKouchak, A., Jézéquel, A., Mahecha, M.D. and Maraun, D., 2020. A typology of compound weather and climate events. Nature reviews earth & environment, 1(7), pp.333-347.

Zscheischler, J., Westra, S., Van Den Hurk, B.J., Seneviratne, S.I., Ward, P.J., Pitman, A., AghaKouchak, A., Bresch, D.N., Leonard, M., Wahl, T. and Zhang, X., 2018. Future climate risk from compound events. Nature Climate Change, 8(6), pp.469-477.

Appendix

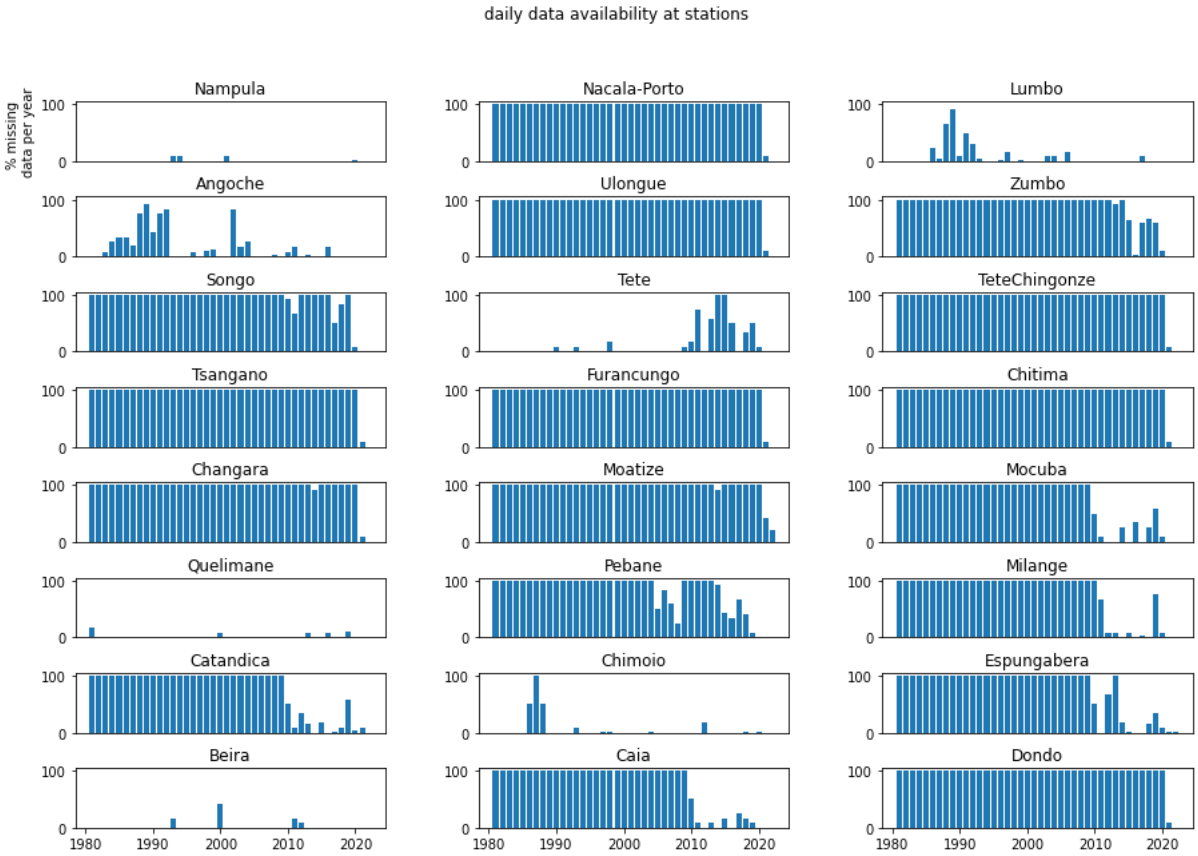

Fig A1. Percentage of missing data for each year in the 1981-2022 period, for 24 weather stations in Mozambique.

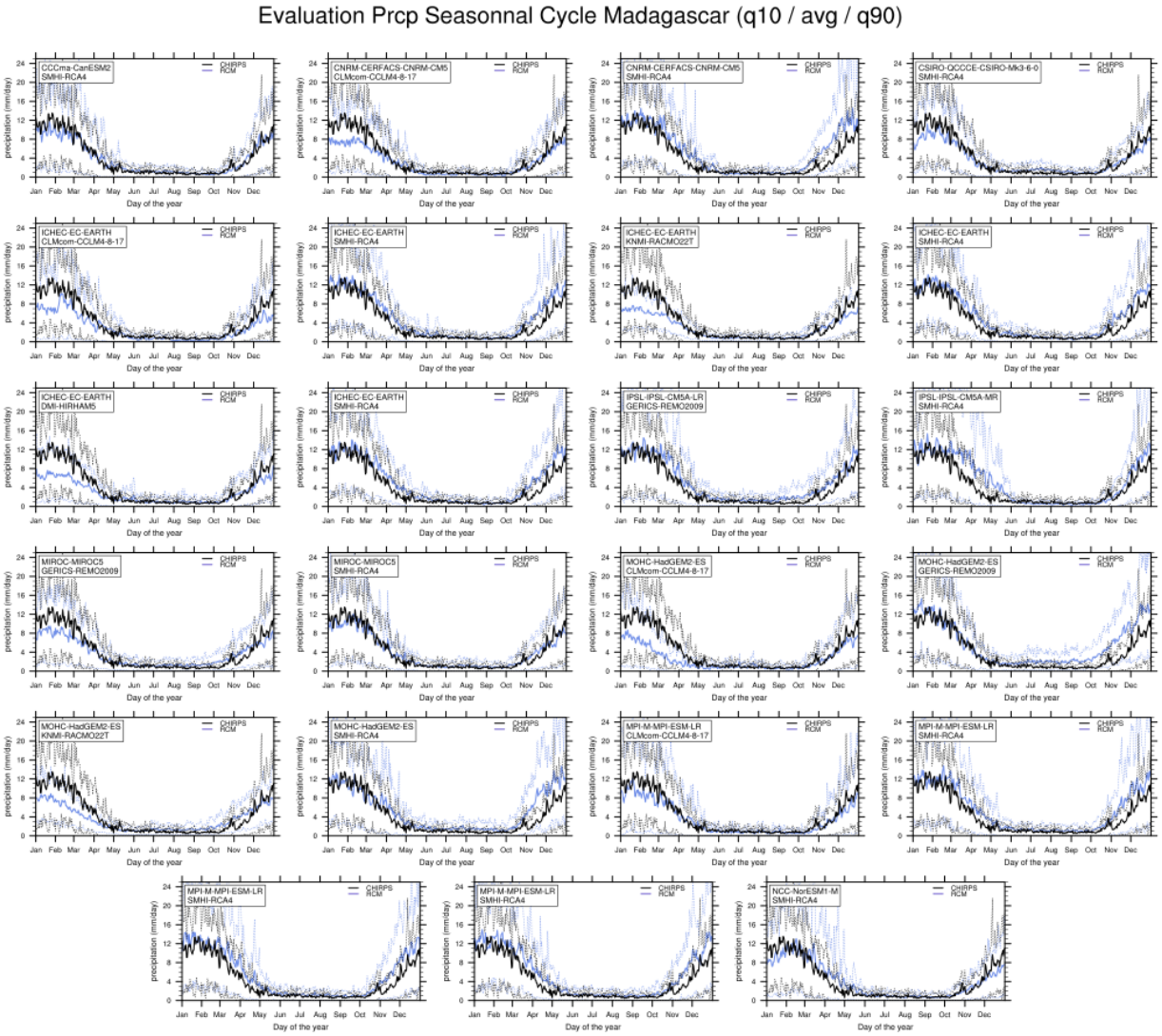

FigA2. Evaluation of annual precipitation cycles from CORDEX models, for Madagascar.

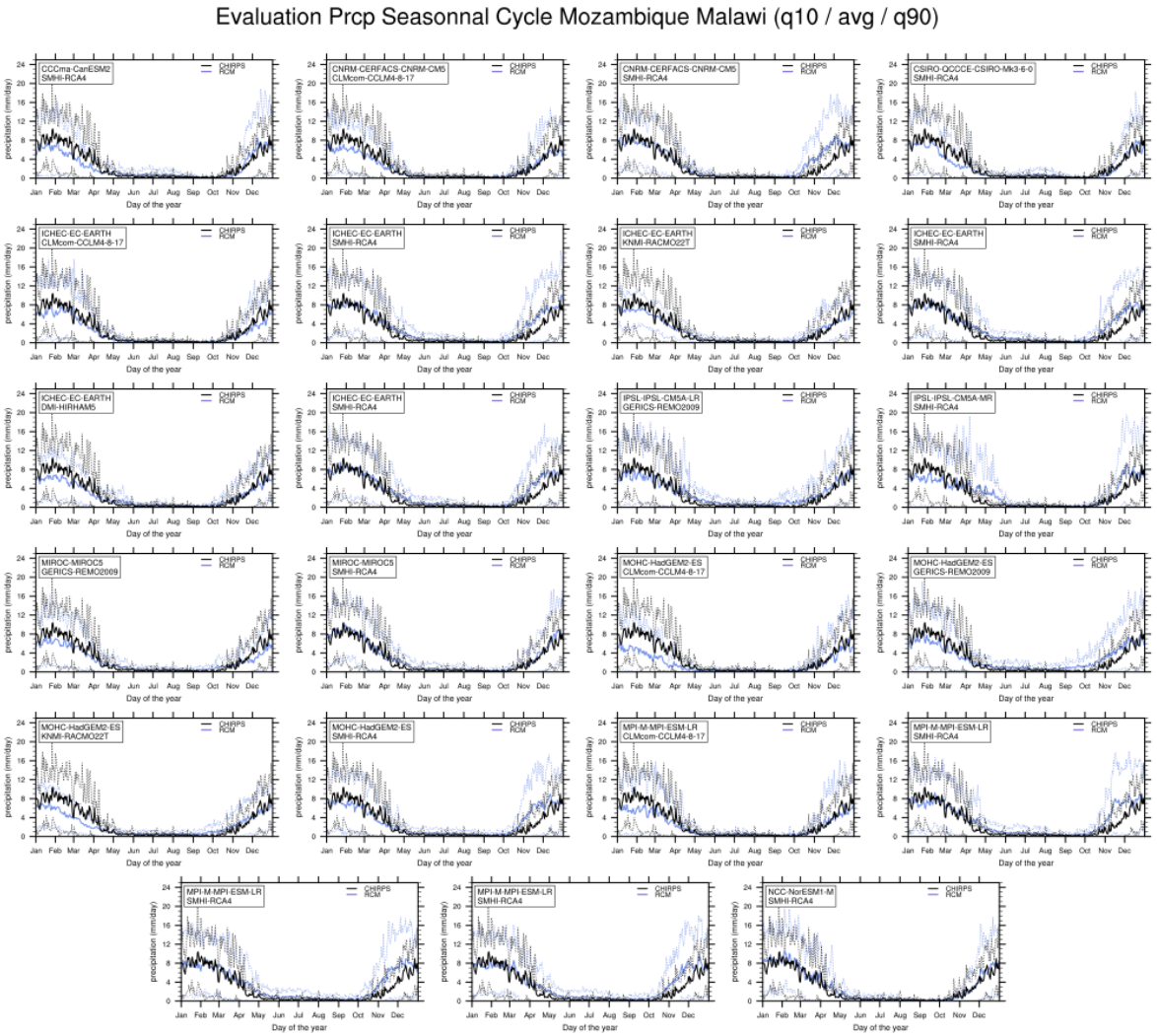

FigA3. Same as Fig. A3, for the MM-box.

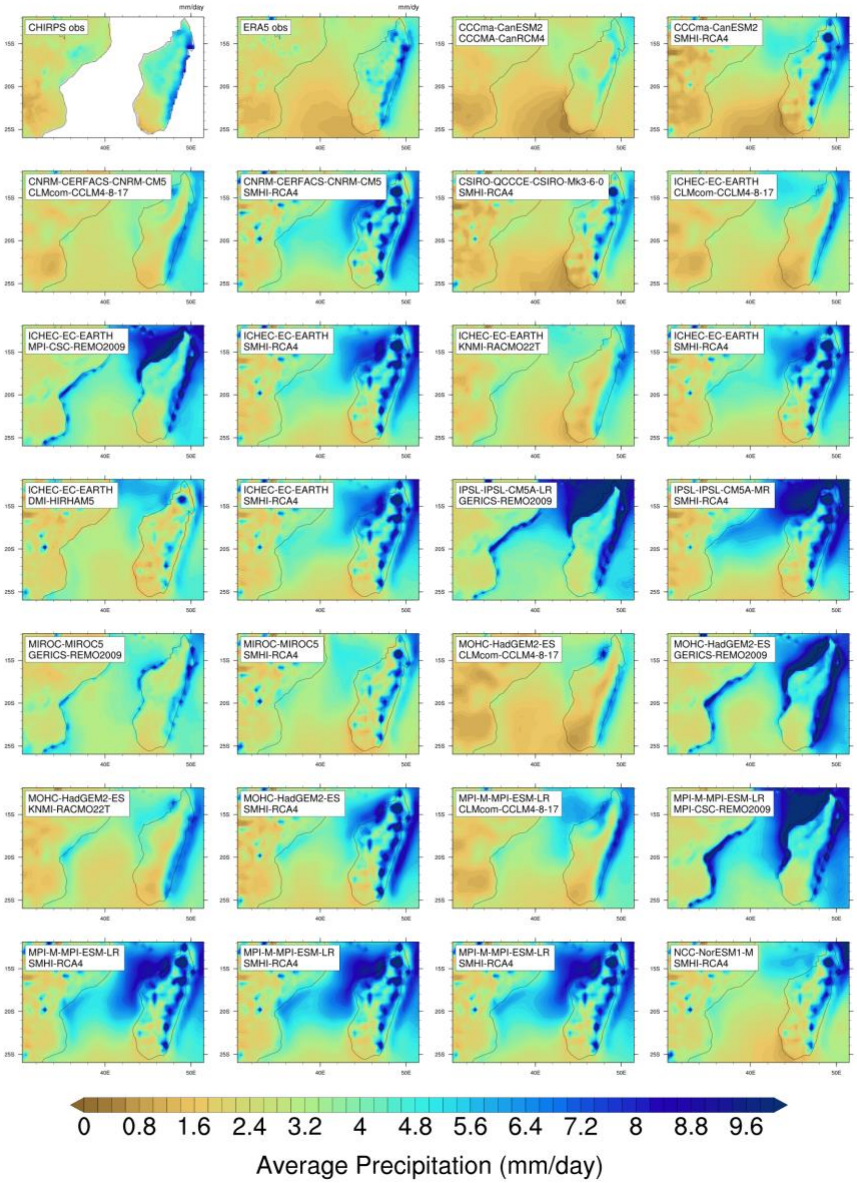

FigA4. Evaluation of average precipitation pattern from the CORDEX models.

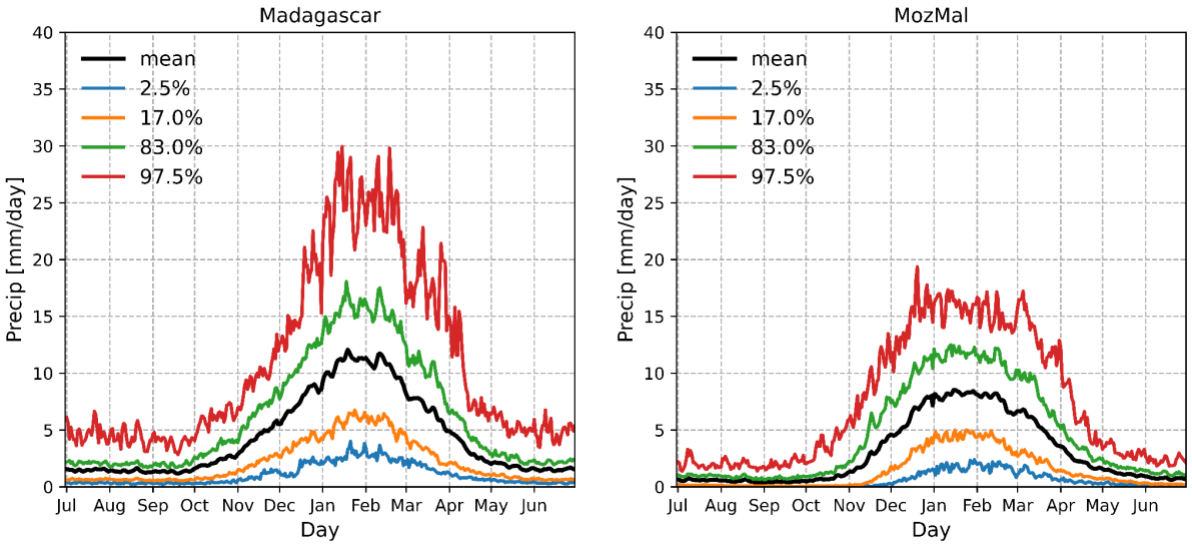

FigA5. Annual precipitation cycle from the coupled FLOR model, for Madagascar (left) and the MM-box (right).

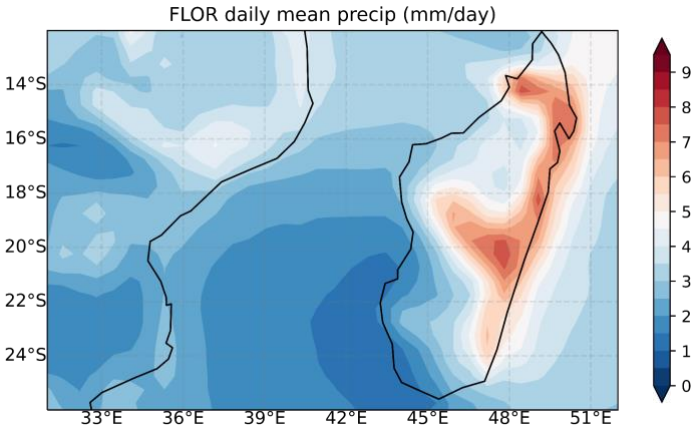

FigA6. Average precipitation pattern from the coupled FLOR model